

APPLICATIONS OF REMOTE SENSING AND
GEOGRAPHIC INFORMATION SYSTEM ON SALINITY
ASSESSMENT: A CASE STUDY ON BANG PAKONG
RIVER, THAILAND



Mr. Min Thura Mon

จุฬาลงกรณ์มหาวิทยาลัย
CHULALONGKORN UNIVERSITY

A Thesis Submitted in Partial Fulfillment of the Requirements
for the Degree of Master of Science in Hazardous Substance and
Environmental Management
Inter-Department of Environmental Management
GRADUATE SCHOOL
Chulalongkorn University
Academic Year 2022
Copyright of Chulalongkorn University

การประยุกต์ใช้ข้อมูลจากการสำรวจระยะไกลและระบบสารสนเทศภูมิศาสตร์เพื่อสำรวจและประเมินค่าความเต็ม: กรณีศึกษาแม่น้ำบางปะกง



วิทยานิพนธ์นี้เป็นส่วนหนึ่งของการศึกษาตามหลักสูตรปริญญาวิทยาศาสตรมหาบัณฑิต
สาขาวิชาการจัดการสารอันตรายและสิ่งแวดล้อม สหสาขาวิชาการจัดการสิ่งแวดล้อม
บัณฑิตวิทยาลัย จุฬาลงกรณ์มหาวิทยาลัย
ปีการศึกษา 2565
ลิขสิทธิ์ของจุฬาลงกรณ์มหาวิทยาลัย

Thesis Title	APPLICATIONS OF REMOTE SENSING AND GEOGRAPHIC INFORMATION SYSTEM ON SALINITY ASSESSMENT: A CASE STUDY ON BANG PAKONG RIVER, THAILAND
By	Mr. Min Thura Mon
Field of Study	Hazardous Substance and Environmental Management
Thesis Advisor	Assistant Professor Dr. SUTHIRAT KITTIPONGVISES
Thesis Co Advisor	Dr Ratchanon Piemjaiswang

Accepted by the GRADUATE SCHOOL, Chulalongkorn University in
Partial Fulfillment of the Requirement for the Master of Science

..... Dean of the GRADUATE
SCHOOL
(Associate Professor Dr YOOTHANA
CHUPPUNNARAT)

THESIS COMMITTEE

..... Chairman
(Professor Dr SRILERT CHOTPANTARAT)
..... Thesis Advisor
(Assistant Professor Dr. SUTHIRAT
KITTIPONGVISES)
..... Thesis Co-Advisor
(Dr Ratchanon Piemjaiswang)
..... Examiner
(Assistant Professor Dr PENRADEE CHANPIWAT)
..... External Examiner
(Professor Dr Chongrak Polprasert)

CHULALONGKORN UNIVERSITY

มิน ทูรา มอน : การประยุกต์ใช้ข้อมูลจากการสำรวจระยะไกลและระบบสารสนเทศภูมิศาสตร์เพื่อสำรวจและประเมินค่าความเค็ม: กรณีศึกษาแม่น้ำบางปะกง. (APPLICATIONS OF REMOTE SENSING AND GEOGRAPHIC INFORMATION SYSTEM ON SALINITY ASSESSMENT: A CASE STUDY ON BANG PAKONG RIVER, THAILAND) อ.ที่ปรึกษาหลัก : สุทธิรัตน์ กิตติพงษ์วิเศษ, อ.ที่ปรึกษาร่วม : รัชชานนท์ เข็มใจสว่าง

ปัญหาความเค็มนับเป็นปัญหาที่สำคัญของแม่น้ำบางปะกงที่พบในทุกปี โดยแม่น้ำบางปะกงเป็นแหล่งน้ำจืดที่สำคัญในเขตระเบียบเศรษฐกิจพิเศษภาคตะวันออกของประเทศไทยและเป็นแหล่งกิจกรรมการเกษตรและอุตสาหกรรม งานวิจัยนี้มีวัตถุประสงค์เพื่อศึกษาและประเมินการกระจายความเค็มในอดีตและอนาคตในแม่น้ำบางปะกงอาศัยการสำรวจระยะไกลและการพยากรณ์อนุกรมเวลาผ่านข้อมูล อนุกรมเวลาของคุณภาพน้ำและการใช้ภาพถ่าย Landsat-8 และการประยุกต์ใช้อัลกอริทึมการเรียนรู้ 4 วิธี ได้แก่ Multilinear Regression, Decision Trees, Random Forest, and Artificial Neural Networks โดยใช้แถบสะท้อนแสงของภาพถ่ายดาวเทียมและค่าความเค็มที่วัดได้ ผลการศึกษาพบว่า Random Forest เป็นโมเดลที่ดีที่สุดด้วยการทำนายผลค่า R^2 ที่สูงกว่าทั้งในข้อมูลดั้งเดิมและข้อมูลที่บูตสแตรป ผลการศึกษายังพบค่าความเค็มสูงสุดมักตรวจพบได้ในเดือนกุมภาพันธ์ ขณะที่เดือนพฤศจิกายนมักพบค่าต่ำสุด นอกจากนี้พบความเค็มเพิ่มขึ้นทุกปีจากแผนที่ความเค็มตามลำดับเวลา โดยเฉพาะบริเวณส่วนปลายแม่น้ำที่มีการเปลี่ยนแปลงความเค็มที่เด่นชัดกว่า (อาทิ จุดตรวจวัดที่ BPK 9.5 ในพื้นที่อำเภอเมืองจังหวัดฉะเชิงเทรา) และการศึกษาวิจัยยังได้ทำนายความเค็มโดยใช้การวิเคราะห์อนุกรมเวลา—Seasonal Auto-regressive Integrated Moving Average (SARIMA) และแบบจำลองโครงข่ายประสาทเทียมแบบถดถอยอัตโนมัติไม่เป็นเชิงเส้น (NARNET) พบว่าแบบจำลอง SARIMA ทำนายค่าความเค็มต่ำสุดและสูงสุดในบริเวณปลายน้ำของแม่น้ำบางปะกงในช่วงเดือนกุมภาพันธ์ ค.ศ. 2024 มีค่าอยู่ในช่วง 14.01 - 63.57 dS/m ในขณะที่พบค่าความเค็มบริเวณต้นน้ำอยู่ในช่วง 1.44 - 16.94 dS/m สำหรับปัจจัยด้านสภาพอากาศ การวิเคราะห์สหสัมพันธ์เพื่อสัมพันธ์พบความสัมพันธ์ผกผันระหว่างปริมาณน้ำฝนและค่าความเค็ม ($r = -0.17$) ในขณะที่พบความสัมพันธ์ในเชิงบวกระหว่างทั้งอุณหภูมิของน้ำ ($r = 0.1$) และอากาศ ($r = 0.22$) กับค่าความเค็ม นอกจากนี้ ข้อเสนอแนะในการจัดการและบรรเทาภัยกับปัญหาความเค็มในแม่น้ำบางปะกงแบ่งออกเป็น 2 ส่วนหลัก ได้แก่ (ก) การบริหารจัดการโดยชุมชนท้องถิ่นและองค์กรบริหารระดับท้องถิ่น และ (ข) การบริหารจัดการโดยหน่วยงานระดับชาติ

จุฬาลงกรณ์มหาวิทยาลัย
CHULALONGKORN UNIVERSITY

สาขาวิชา การจัดการสารอันตรายและสิ่งแวดล้อม
ปีการศึกษา 2565

ลายมือชื่อนิติสด
ลายมือชื่อ อ.ที่ปรึกษาหลัก
ลายมือชื่อ อ.ที่ปรึกษาร่วม

6388527220 : MAJOR HAZARDOUS SUBSTANCE AND ENVIRONMENTAL MANAGEMENT

KEYWORD: Bang Pakong river, Salinity, Remote Sensing, Time Series Forecast

Min Thura Mon : APPLICATIONS OF REMOTE SENSING AND GEOGRAPHIC INFORMATION SYSTEM ON SALINITY ASSESSMENT: A CASE STUDY ON BANG PAKONG RIVER, THAILAND. Advisor: Asst. Prof. Dr. SUTHIRAT KITTIPONGVISES Co-advisor: Dr Ratchanon Piemjaiswang

The Bang Pakong River (BPK) has an annual salinity issue. The river is an important source of freshwater supply in the Eastern Economic Corridor (EEC) of Thailand, which has major agricultural and industrial activities. This research aims to understand and assess the past and future salinity distribution in the BPK River by using remote sensing and time series forecasting through water quality and Landsat image time series data. Regarding to remote sensing, this research employs four machine learning algorithms—multilinear regression, decision trees, random forest, and artificial neural networks—by applying reflectance bands of satellite images and measured salinity values. Random forest is the best model with higher R^2 and lower RMSE in both original and bootstrapped data, indicating the model of choice for salinity study. It is also noted that the salinity increases annually which is evident from the time sequence salinity maps, in particular, the downstream part has more prominent salinity changes, especially to BPK9.5 (Mueang Chachoengsao District). Compared to two Time Series Analysis—Seasonal Autoregressive Integrated Moving Average (SARIMA) and Nonlinear Autoregressive Neural Network (NARNET) Model, in which SARIMA model can predict the salinity with lower RMSE. Based on the forecasted salinity values of SARIMA, maximum and minimum salinity of downstream part in February 2024 is 63.57 - 14.01 dS/m, while in the upstream part, the range of 16.94 - 1.44 dS/m is observed. As regard to climate factors, precipitation and the salinity have the inverse relationship with -0.17 of Pearson correlation coefficient. In addition, temperatures of both water and atmosphere have fair correlations: 0.22 (air) and 0.1 (water) with salinity. However, the water level has no relationship with the salinity, in which Pearson correlation value is 0.01 with EC and -0.02 with TDS respectively. Moreover, the suggestions for salinity prevention are discussed in two main parts: (a) Capability within the local community and administrative body and (b) Capability at the national level.

จุฬาลงกรณ์มหาวิทยาลัย
CHULALONGKORN UNIVERSITY

Field of Study: Hazardous Substance and Environmental Management
Academic Year: 2022

Student's Signature

Advisor's Signature

Co-advisor's Signature

ACKNOWLEDGEMENTS

I would like to thank the International Program on Hazardous Substances and Environmental Management (IP-HSM), Graduate School of Chulalongkorn University for the research funding. I am very grateful to my advisor, Assistant Professor Dr.Suthirat Kittipongvises for guiding me step by step to make this research successful and giving me a chance to learn many new things from this research work. In addition, I am very indebted to my co-advisor, Dr Ratchanon Piemjaiswang for insightful and critical comments and guidance throughout this research journey. I am very thankful to my thesis committee chair: Professor Dr Srilert Chotpantararat, committee member: Assistant Professor Dr Penradee Chanpiwat and external committee member: Professor Dr Chongrak Polprasert for their valuable insights and suggestions on this research work. In addition, I acknowledge the Pollution Control Department Thailand and the United State Geological Survey (USGS) for their contribution in terms of data. I do appreciate to my family, and close friends for their unwavering support all over the course of my academic journey.

Min Thura Mon



จุฬาลงกรณ์มหาวิทยาลัย
CHULALONGKORN UNIVERSITY

TABLE OF CONTENTS

	Page
ABSTRACT (THAI)	iii
ABSTRACT (ENGLISH).....	iv
ACKNOWLEDGEMENTS.....	v
TABLE OF CONTENTS.....	vi
List of Figures	1
List of Tables	3
CHAPTER 1	4
1.1 Problem Statement.....	4
1.2 Research Objectives	5
1.3 Research Questions	6
1.4 Scope of Study.....	6
1.5 Expected Outcome.....	6
CHAPTER 2	7
2.1 Remote Sensing Application on Surface Water and Salinity Intrusion	7
2.2 Landsat-8 Application and Processing for Water-related Studies.....	8
2.3 Machine Learning Application.....	8
2.3.1 Multiple Linear Regression	8
2.3.2 Decision Trees	9
2.3.3 Random Forest	9
2.3.4 Neural Network	9
2.3.5 Bootstrap Method	9
2.4 Time Series Analysis on Salinity Prediction	10
2.4.1 Seasonal Auto-regressive Integrated Moving Average Model	10
2.4.2 Nonlinear Auto-regressive Neural Network Model	11
2.5 Previous Studies	12

2.5.1 Previous studies related to water quality and ecological studies of the BPK River	12
2.5.2 Previous studies on Remote Sensing application for salinity assessment	14
CHAPTER 3	16
3.1 Study Area	16
3.2 Data collection	16
3.2.1 Landsat-8 Data Collection and Processing.....	16
3.2.2 Detecting Water Area from Landsat-8	17
3.2.3 Water Quality Time Series Data	17
3.3 Model Development for Remote Sensing.....	18
3.3.1 Preparation of Reflectance Wavelength - Bands Data	19
3.3.2 Salinity Modelling with Reflectance Wavelength.....	19
3.3.3 Resampling by Bootstrap Data.....	19
3.3.4 Salinity Modelling with Reflectance Wavelength Using Bootstrap Data	19
3.3.5 Data Validation.....	21
3.4 Time Series Prediction on Salinity	22
3.4.1 SARIMA and NARNET Models	22
3.4.2 Data Evaluation	23
3.5 Salinity Mapping	23
CHAPTER 4	24
4.1 Assessing Salinity via Remote Sensing and GIS Methods.....	24
4.1.1 Relationship between the reflectance and salinity	24
4.1.2 Salinity Modelling with Original Data	25
4.1.3 Salinity Modelling with Bootstrap Data.....	31
4.1.4 Salinity Mapping	33
4.2 Assessing Salinity via Time Series Methods.....	41
4.2.1 Results of SARIMA Model	41
4.2.2 Results of NARNET Model	43
4.2.3 Discussions on Time Series Models.....	45

4.3. Investigation of Climate and Water-related Factors on Salinity	47
4.4 Recommendations on Salinity	49
4.4.1 Suggestions on Salinity Prevention	49
4.4.2 Limitation of Research	51
CHAPTER 5	54
REFERENCES	57
ANNEX.....	66
VITA.....	68



List of Figures

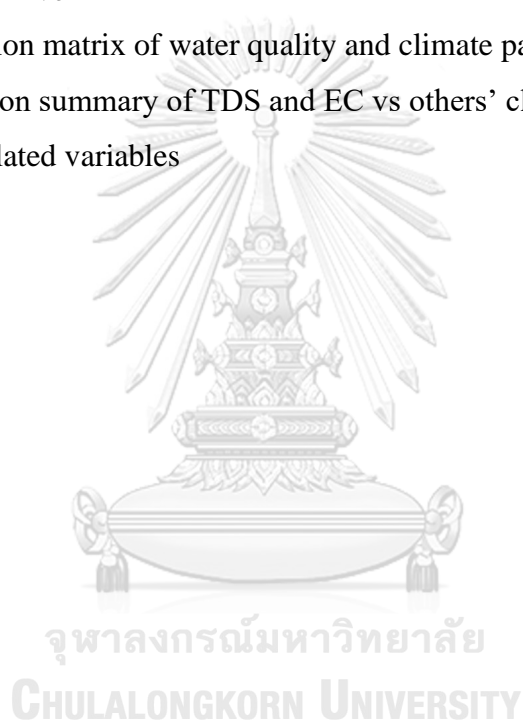
	Page
Figure 2.1 Example of bootstrap method	10
Figure 2.2 NAR network schematic structure (Hadiyan, Moeini and Ehsanzadeh, 2020)	12
Figure 3.1 Location and sampling site map of Bang Pakong River	18
Figure 3.2 Research methodology flow chart	20
Figure 4.1 Multiple linear analysis of the relationship between salinity & composite bands.	24
Figure 4.2 Composite band 247 on (A) February 2nd, 2020, and (B) February 5th, 2021	26
Figure 4.3 Composite band 234 on (A) February 2nd, 2020, and (B) February 5th, 2021	27
Figure 4.4 Regression of MLR and DT using the original data as 70% training, 15% testing and 15% validation	28
Figure 4.5 Regression of RF using the original data	29
Figure 4.6 Regression of ANN using the original data	30
Figure 4.7 Comparison of R2 and RMSE in training, testing and validation of models with original data (O = 282 samples) and bootstrap data (B*2 = 564 samples and B*4 = 1128 samples)	32
Figure 4.8 Salinity Map of BPK in February 2018	35
Figure 4.9 Salinity Map of BPK in February 2019	36
Figure 4.10 Salinity Map of BPK in February 2020	37
Figure 4.11 Salinity Map of BPK in February 2021	38
Figure 4.12 Salinity variation of BPK downstream part from 2018 to 2021	39
Figure 4.13 Salinity variation of BPK upstream part from 2018 to 2021	40
Figure 4.14 Observed salinity in February along the main BPK river	41
Figure 4.15 ACF and PACF plots of ARIMA models from each group, starting from BPK01 to BPK11	42
Figure 4.16 Comparison of MSE vs numbers of hidden layers	43

	Page
Figure 4.17 Performance plot of NARNET at selected stations	44
Figure 4.18 Comparison of salinity values of SARIMA, NARNET and measured at the mid and upstream part of the BPK river.	45
Figure 4.19 Comparison of salinity values of SARIMA, NARNET and measured at the downstream part of the BPK river	46



List of Tables

	Page
Table 2.1 Applications of remote sensing and GIS in water and salinity related studies	7
Table 3.1 Framework for defining and mapping salinity	23
Table 4.1 Classification of saline water	34
Table 4.2 Statistics of each selected station along the BPK River	42
Table 4.3 NARNET model parameters of each selected station along the BPK River	43
Table 4.4 Correlation matrix of water quality and climate parameters	47
Table 4.5 Regression summary of TDS and EC vs others' climate and water-related variables	47



CHAPTER 1

INTRODUCTION

1.1 Problem Statement

The Bang Pakong River (BPK) is facing with salinity problem annually. On top of that, BPK River is an agriculturally and industrially important source of freshwater supply in the Eastern Economic Corridor of Thailand (Chaiyarak, Tattiyakul and Karnsunthad, 2019). Salinity intrusion is an environmentally challenging matter for the supply of freshwater in the coastal areas, especially in Southeast Asia (Himi *et al.*, 2017). Salinity is an even more important parameter in quality of freshwater particularly for irrigation purpose. In addition, there is a potential inflow of saltwater into the river through the estuary from the Gulf of Thailand. Salinity influences outputs of crops, and trees by causing dehydration of plants, restricting uptake of nitrogen, diminishing growth, and interrupting plant propagation. Particular ions, specifically chloride, are lethal to plants. Hence, when an increase in intensity of these ions, the plant is contaminated and goes dead.

Total dissolved solids (TDS) comprise of all the substances of both organic and inorganic which are dissolved in water. Sodium, calcium, potassium, magnesium, chloride, sulphate, bicarbonate, nitrate, as well as silica usually comprise of major dissolved solids in water. Through the combination of ions, such as chloride and sodium lead to the formation of salts. Thus, salinity is an alternative term, used to describe the dissolved solids content of water (USGS, 2019). The concentrations of TDS in water may be so high that the water is not suitable for irrigation, drinking, and other uses. If the concentration is greater than the recommended value of 500 mg/L in drinking water, the water will have an unpleasant salty taste (USGS, 2019). In terms of health impact, the concentration of chloride, a major component of TDS, is typically negligible and is not an issue in normal drinking water. However, a matter is the continuing cancer risk due to chronic introduction to chlorinated water. The main reason is trihalomethanes (THM) and other disinfection by-products of the chlorination. THMs are carcinogens, and chlorinated water has linked along with bladder, colon, and rectal cancer risks (USEPA, 2022). In extreme concentrations of TDS in water supply system, it will cause corrosion of plumbing fixtures and reduction in lifespan of equipment of water distribution systems.

The degree of salinity is a complicated issue subject to several factors for instance, upstream freshwater flow, geomorphology and channel size, tidal situations, and existence of control structures (Nguyen *et al.*, 2008). The capacity to forecast intrusion of salinity was a matter of concern in various preceding findings. Hydraulic models also considered being as a mean in stimulating intrusion of saline water in delta areas. Nevertheless, former models remain intricate and require substantial collection of data, which rely on comprehensive topographic and up-to-date infrastructure information.

On the contrary, distant detection techniques create innovative uses to examine ocean, surface water, and coastal salinity. The achievement of remotely sensed data for calculating saline intrusion have been proved in prior investigations employing Landsat Thematic Mapper (Loc *et al.*, 2021; Nguyen *et al.*, 2021), Moderate-resolution Imaging Spectroradiometer (MODIS) (Urquhart *et al.*, 2012). In addition, when water is exposed to pollution or impurities, a change in TDS increases the level of electrical conductivity (EC). Thus, EC can also be an indicator of salinity especially for saline water that shows high to very high EC readings. This is because when salt is dissolved, it separates into ions.

Nonetheless, in the case of BPK, only a very few previous studies had used Remote Sensing and Geographic Information System (GIS) as well as Time Series Methods to assess the salinity of freshwater in the BPK River. This condition makes the research gap on the salinity study of the BPK River, which in term creates a problem of lacking data in preparing for future climate change induced water-related issues, especially salinity intrusion. Thus, from this study, this research covers the information gap in salinity variation, provide future salinity and correlate the salinity with historical climate factors and water levels based on an approach using Remote Sensing and GIS, supported by machine learning methods, thereby enhancing the understanding on spatiotemporal variation of salinity for developing an effective salinity management strategy.

1.2 Research Objectives

Primary aim of this research study is to understand and assess the past and future salinity distribution in the BPK River by using remote sensing and time series

forecasting through time series data of water quality and Landsat-8 images. Specific purposes are given as follows:

- (a) To understand the salinity variation in the BPK River based on remote sensing methods and forecast future salinity using Time Series Analysis.
- (b) To investigate the impact of climate related factors on salinity occurrence in the BPK river.
- (c) To provide potential recommendations on salinity preventive measures.

1.3 Research Questions

In this study, the following three research questions were investigated: (a) What is the variation of salinity distribution and future salinity of the BPK River? (b) What are main factors among historical climate factors namely, temperature, precipitation, and water level that influence the salinity? (c) What kinds of recommendations and suggestions can be made for preventing salinity problems?

1.4 Scope of Study

This study focused on the current salinity distribution in BPK River, prediction of future river salinity, correlation with both historical climate parameters, i.e., temperature, precipitation, and water level, as well as recommendations for salinity preventive measures.

1.5 Expected Outcome

This study provides many useful information on the past salinity variations, future salinity, influencing climate and water level parameters on salinity of the BPK River. The information from this study can be applicable not only for hydrologists and scientists for further studies but also for policymakers and general experts in drafting salinity preventive measures as salinity can impact the agriculture, irrigation, and public health.

CHAPTER 2

LITERATURE REVIEW

2.1 Remote Sensing Application on Surface Water and Salinity Intrusion

Remote sensing methods were extensively employed in detecting freshwater bodies with a great accuracy on a global scale (Kumar and Reshmidevi, 2013). Furthermore, high-resolution remotely sensed data generates greater applicability by establishing timely and trustworthy measurements of local water and land features (Sawaya *et al.*, 2003). Choosing proper images differ on goals, commercial conditions, and attributes of each case study. In determining suitable satellite images, spatial resolution of satellites (10-60 m in Sentinel, 30 m in Landsat, 250-1000 m in MODIS) and frequency of satellite orbit (Landsat: each 16 days, Sentinel: each 5 days, MODIS: each 1-2 days) are the key considerations in the study. The following studies in Table 2.1 indicate the various applications of remote sensing, based on distinct satellite data.

Table 2.1 Applications of Remote Sensing and GIS in Salinity and Water Related Studies

Satellite Images	Specific Applications in Water and Salinity related studies
Landsat	Salinity intrusion prediction (Nguyen <i>et al.</i> , 2021)
	Water salinity mapping (Ansari and Akhoondzadeh, 2019)
	Sea surface salinity (J. Zhao, Temimi and Ghedira, 2017)
Sentinel	Sea level salinity in estuary zone (Tunjung <i>et al.</i> , 2021)
	Soil salinity mapping (Morgan, El-Hady and Rahim, 2018)
	Studies of human impacts on coastal water (Vanhellemont and Ruddick, 2014)
MODIS	Surface water turbidity (Constantin, Constantinescu and Doxaran, 2017)
	Sea surface salinity (E.A. Urquhart <i>et al.</i> , 2012)

GIS and remote sensing practices has been used extensively to applications of observing water conditions (Xiao *et al.*, 2018), detecting water volume such as

flooding (Ma, Guo and Zhou, 2013), and evaluating impacts of water discharge soon after mixing up of freshwater and seawater in coastline. (Wang, F. and Xu, 2008).

2.2 Landsat-8 Application and Processing for Water-related Studies

The Landsat-8 has excellent possibility for various uses in land cover, water, and change detections (Roy *et al.*, 2014). Moreover, the resolution Landsat-8 images stay powerful and appropriate to employ in estuarine and coastal water environments (Vanhellemont and Ruddick, 2014). Appendix 1 indicates the resolution and wavelength of total 11 bands in Landsat-8 OIL and TIRS (U.S. Geological Survey, 2019). Landsat-8 comprises of 11 bands, and each individual band has strength and limitations for each field of application (Acharya, 2015).

Composition of image bands is a suitable approach to display common characteristics of one object. Pattern of diverse bands can have an advantage to unrelated graphical features comparative to physical properties of the wavelength. According to (UC Berkeley, 2008), Bands 3,2,1: this colour combination is near to the true colour and valuable for aquatic habitats research. Bands 4,3,2: it displays comparable qualities to bands 3,2,1 image but due to the NIR band, water-land boundaries are sharper as well as numerous kinds of flora becomes evident.

2.3 Machine Learning Application

Machine learning (ML) can be utilized to distinguish data patterns, fused computer science with mathematical methods (Stephen, 2007). ML contains supervised learning: input data as training data while an output as target, and unsupervised learning: no target output is provided. The following Machine Learning Models are commonly used in salinity prediction of water resources.

2.3.1 Multiple Linear Regression

Multiple linear regressions (MLR) are the most functional arithmetical models (Owen, 2001). MLR is straightforward and frequently offer a satisfactory and understandable narrative of how inputs affect output (Hastie, Tibshirani and Friedman, 2009).

2.3.2 Decision Trees

Decision Trees (DT) classification begins with a whole set of existing training samples, in which recursive binary partition is made for each point till a particular ending criterion is contented. A tree chart with the stems formed by the split laws and a sequence of final nodes are observed as that encompass a mean response (Basu and Basu, 2011).

2.3.3 Random Forest

Random Forest (RF) is employed by developing trees on a random vector. The tree predictor takes on statistical values as countered to group descriptions (Breiman, 2001). This randomization resulted from bootstrapping a sample from the training set and randomly choosing entry predictors to split on at each node. Out-of-bag refers to the non-selected situations. (Epifanio, 2017a).

2.3.4 Neural Network

Prior to training, the neural network must specify parameters including the number of responses, layers, and output connections. To prevent early stops that could reduce the model's performance, the training algorithm that is chosen is of the utmost importance. For training small and medium-sized networks and patterns, the Levenberg-Marquardt is appropriate. (Hastie, Tibshirani and Friedman, 2009).

2.3.5 Bootstrap Method

Bootstrapping is a resampling technique that allows for the creation of statistical inferences from data without taking into account the original data's robust distributional assumptions (Haukoos and Lewis, 2005; Dixon, 2006). Any statistical analysis with a small sample size raises problems, and model predictive power is reduced (Stockwell and Peterson, 2002; McPherson, Jetz and Rogers, 2004). Therefore, a larger dataset should improve model performance.

Through random sampling with replacement, bootstrap samples are generated from the original dataset (Wehrens, Putter and Buydens, 2000). Each bootstrap sample must have the same sample size as the original data set in order for the computed confidence interval to be approximate and free of bias problems (Haukoos

and Lewis, 2005). The original training sample serves as the test sample, and the bootstrap datasets serve as the training samples. Both samples produce similar results (Hastie, Tibshirani and Friedman, 2009).

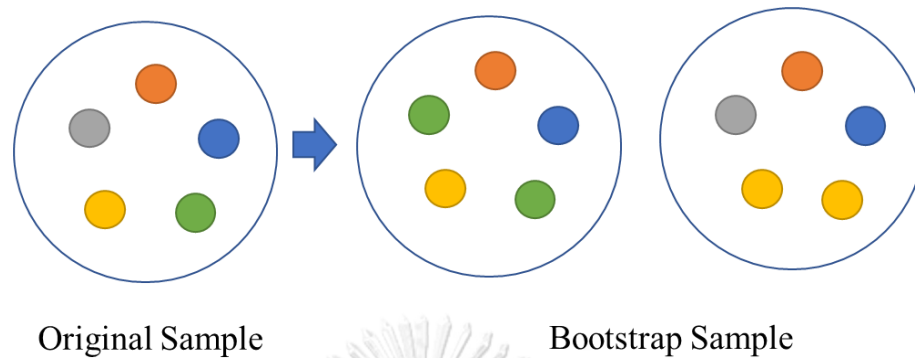


Figure 2.1 Example of bootstrap method

2.4 Time Series Analysis on Salinity Prediction

All of the prediction models rely heavily on historical data. To create prediction models, long-term data from historical values is required. However, when the data are noisy and the historical value data are few, the likelihood of incorrect forecasts will rise (Lin et al., 1996). Further, these methods based on historical time series data assume that the past data will appear in the future (Notton and Voyant, 2018; Rouchier, Rabouille and Oberlé, 2018).

2.4.1 Seasonal Auto-regressive Integrated Moving Average Model

Box-Jenkins-based time series stochastic models are used for the time series analysis on salinity prediction (Lorek et al., 1976). The time series' stationary state had to be established before its seasonality could be examined in order to create a Box-Jenkins model (Hipel, McLeod and Lennox, 1977). In order to improve the stationarity of the data by removing any potential trends, a second-order differencing method is used. In (Eq. 1), the second-order differencing is termed:

$$\Delta^2 y_t = y_t - 2y_{t-1} + y_{t-2} \quad (1)$$

Since salinity values still show seasonality after differencing, Seasonal auto-regressive integrated moving average (SARIMA) model is able to be applied. The autocorrelation function (ACF), partial autocorrelation function (PACF), and

Bayesian information criterion (BIC) are used to determine the orders of the SARIMA model (Wei and Hillmer, 1991). The SARIMA general formula is provided in (Eq.2).

$$\text{SARIMA}(p,d,q)(P,D,Q)_s : \varphi_p(B)\Phi_p(Bs)\nabla^d\nabla^D s y_t = \theta_q(B)\Theta Q(Bs)\varepsilon_t \quad (2)$$

where, y_t is the time series value at time t and φ , Φ , θ and Θ are polynomials of order of p , P , q and Q respectively. The trend elements are p : trend autoregression order, d : trend difference order, q : trend moving average order as part of the trend elements, and the seasonal elements P : seasonal autoregressive order, D : seasonal difference order, Q : seasonal moving average order and s : the number of time steps for a single seasonal period. B is the backward shift operator and $\nabla = (1 - B)$. White noise is denoted by ε_t .

2.4.2 Nonlinear Auto-regressive Neural Network Model

Typical time series models are linear models, like ARIMA (Auto-Regressive Integrated Moving Average). A nonlinear model should be suggested for time series since time series in all applications are sensitive to significant variations and quick transients cannot be modelled by a linear model. Another model (Ibrahim et al., 2014) is described with this focus in mind in (Eq.3).

$$\Delta_{y-1}^d = h(\Delta_{y-1}^d, \Delta_{y-2}^d, \dots, \Delta_{y-p}^d, \varepsilon_{t-1}, \dots, \varepsilon_{t-q}) + \varepsilon_t \quad (3)$$

where $\Delta_{y-1}^d = (1 - B^d) y_t = y_t - y_{t-d}$ is the differentiation operator, B^d is the delay operator and h is an approximation nonlinear function. Based on (Lapedes and Farber, 1987), it was proved that time series can always be modelled by the following nonlinear, autoregressive (NAR: Nonlinear Auto-Regressive) model that is formulated in (Eq.4).

$$y(t) = h(y(t-1), y(t-2), \dots, y(t-p)) + \varepsilon(t) \quad (4)$$

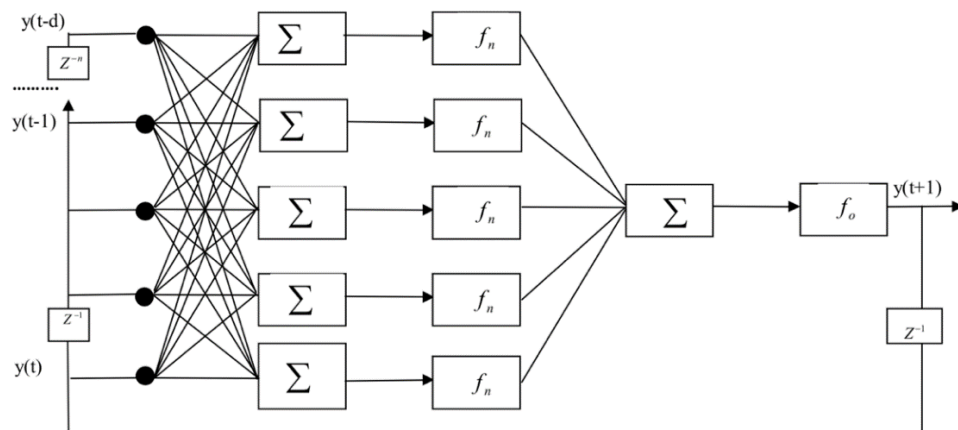


Figure 2.2 NAR network schematic structure (Valipour, Banihabib and Behbahani, 2013; Hadiyan, Moeini and Ehsanzadeh, 2020)

As illustrated in Figure 2.2 is a multilayer, recurrent, dynamic network, with feedback connections (AL-Allaf and AbdAlKader, 2011). The propagation algorithm's gradient descent serves as the foundation for the learning rule. The following reasoning can be used to justify the decision to use the NARNET: When dealing with issues involving long period reliance, the classical recurrent network has some issues, especially when dealing with time series (Temurtas et al., 2004). In the current study, NARNET is the network of choice because fluctuations in salinity levels necessitate a model with quick time series prediction in order to develop a real-time application.

2.5 Previous Studies

2.5.1 Previous studies related to water quality and ecological studies of the BPK River

Regarding on the previous studies of BPK river, temperature, dissolved oxygen, turbidity, suspended particles, pH, ammonia, faecal coliforms, chemical and biological oxygen demand, conductivity, phosphate, and heavy metals were all examined by (Bordalo, Nilsumranchit, and Chalermwat, 2001) between June 1998 and May 1999. They came to the conclusion that the average WQI was low (41%) and that the dry season had a substantial negative impact on quality.

The BOD, total, and faecal coliform bacteria levels, together with sporadic high levels of Pb, Hg, Cd, and Mn, were much higher than the regulatory limits for

surface water quality, according to a comparable water quality assessment of the BPK River by (Bubphamala, Benjawan, and Liamlaem, 2010). Compared to the wet season, the severity of the pollution appeared to be higher in the dry season. The dry season is also when excessive salinity is often seen. Salinity intrusion is a major issue for the BPK river basin, according to several studies on the BPK river (Promchote, 2009; Chaiyarak, Tattiyakul, and Karnsunthad, 2019).

Kupkanchanakul et al., in 2015 used mathematical material flow and geographical land use analysis to pinpoint the location of the sources and processes of nitrogen and phosphorus in the BPK area (Kupkanchanakul et al., 2015). According to their findings, rice and aquaculture both use fertilizers and feeds to produce significant levels of nutrient inputs. On the other hand, perfluorinated compounds (PFCs), particularly perfluorooctane sulfonate (PFOS) and perfluorooctanoic acid (PFOA), were found at lower concentrations in the BPK River, with average concentrations of 0.7 ng/L for both PFOS and PFOA.

According to the report of Bang Pakong River Basin Committee by (Molle, Srijantr and Promchote, 2009), the BPK river is characterized by relatively high rainfall, very little runoff during the dry season, a low capacity for water storage, significant aquaculture and irrigated land areas, industrialization hotspots, and challenges managing and preventing saltwater intrusion. As an ecological, fate and transport study of BPK area, emphasising on risk of antibiotics from pig farms, (Chan *et al.*, 2020) conducted the research on the fate, transport, and ecological risk of antibiotics drained from pig farms along the BPK river in dry and rainy seasons of 2018.

There are also some studies focused on salinity prevention in terms of dam construction by considering the interactions between tide and salinity barrier; (Vongvisessomjai and Srivihok, 2003) conducted the analytical model by using MIKE-11, but later, (Vongvisessomjai, Chatanantavet and Srivihok, 2008) pointed out the numerical model was lack of consideration on the effects of barrier construction in creation of reflected tide.

2.5.2 Previous studies on Remote Sensing application for salinity assessment

In terms of the application of remote sensing on salinity, (Nguyen *et al.*, 2021) and (Nguyen, 2018) conducted the salinity intrusion prediction using remote sensing and machine learning approach in Vietnam's Mekong Delta that is data limitation problem. Numerous algorithms had been implemented to find the best solution for this issue, including Xgboost, Gaussian processes, support vector regression, deep neural networks, grasshopper optimization algorithm, random forest, and decision trees.

Moreover, research conducted by (Tran *et al.*, 2021) studied the hydrological drivers of saltwater intrusion in Vietnamese Mekong Delta. They examined how the hydrological drivers shape the adaptation strategies of rural communities in the coastal areas by using mixed sources of historical measured data, numerical modelling, and qualitative data. Plus, (Tran *et al.*, 2019) examined spatiotemporal salinity dynamics in the Mekong River Delta using Landsat time series imagery and a spatial regression approach. In addition, a study of (Wassmann *et al.*, 2019) considered flood and salinity risks for rice production in the Vietnamese Mekong Delta via high-resolution mapping approach.

By using remote sensing techniques, some studies (Ansari and Akhoondzadeh, 2020) also learnt the water salinity through regression models to ascertain the water salinity through the connection between Landsat-8 OLI's reflectance and field measurements in Iran. In addition, (Ali Khan *et al.*, 2022) applied the random forest algorithm for modelling of surface water salinity in terms of electrical conductivity and TDS in the upper Indus River basin, India.

Besides this, (Al Shehhi and Kaya, 2021) evaluated the performance of stochastic time series models - Seasonal Auto Regressive Integrated Moving Average (SARIMA) and nonlinear neural network (NN) - to predict surface chlorophyll- α (Chl- α) and sea surface temperature (SST) in coastal areas. Moreover, (Kbaier Ben Ismail, Lazure and Puillat, 2016) observed the statistical properties and time-frequency analysis of temperature, salinity and turbidity in the coastal waters of Boulogne-Sur-Mer, France.

Apart from SARIMA, (Ibrahim *et al.*, 2016) studied a new real time energy management strategy using a Nonlinear Auto-Regressive Neural Network (NARNN)

as a time series prediction model, and Discrete Wavelet Transform (DWT) as a time-frequency filter. Furthermore, (Hadiyan, Moeini and Ehsanzadeh, 2020) also used different models of static and dynamic artificial neural networks (ANN) including static feed forward neural network (FFNN), non-linear autoregressive (NAR), and nonlinear autoregressive with exogenous inputs (NARX) are employed to forecast Sefidroud Dam reservoir inflows in Iran.



CHAPTER 3

RESEARCH METHODOLOGY

3.1 Study Area

The Bang Pakong River Basin connects to the Gulf of Thailand and has a total area of 10,707 km² (1.07 million acres). The Sankamphaeng Mountains, Dong Phrayayen - Khao Yai Mountains, and Chanthaburi Mountains are the source of the basin catchment in the north and east, respectively. The two principal rivers, Prachinburi River and Nakhon Nayok River, originate in Khao Yai National Park and merge to form the Bang Pakong River in Yothaka Subdistrict of Chachoengsao Province (Figure 3.1) (Chaiyarak, Tattiyakul and Karnsunthad, 2019). In this study, the research focused only on the main Bang Pakong River area.

The BPK River that flows through Chachoengsao, Chonburi, Prachinburi and Nakhon Nayok Provinces, with a total length of 122 km and an elevation range of 0 – 20 m above sea level. The monsoon season is usually from May until late September, with averagely 1-2 tropical depressions occur over much of the area. The average annual rainfall is 1,387 mm, depending on monsoon direction and elevation with the maximum average in September. The river basin is characterized by rapid industrialization and having one of the most pressing water problems in Thailand.

Although it is a significant ecological feature, the deep inflow of seawater into the Bang Pakong River during high tides and the dry season also has an impact on farming operations in the basin. A dam was built close to Ban Phai Saweang in the Bang Kaew Subdistrict of Chachoengsao to safeguard the area from seawater intrusion and to store freshwater for use during the dry season. On January 6, 2000, the dam went into service. Since then, however, it has generated a number of issues and is no longer in use. The dam's opening and closure have caused various issues and disputes in some places, despite the fact that it was built to prevent saltwater incursion in the event of high seawater levels. (Chaiyarak, Tattiyakul and Karnsunthad, 2019).

3.2 Data collection

3.2.1 Landsat-8 Data Collection and Processing

Landsat-8 has a whole areal coverage each 16 days and 30-meter spatial resolution. A total of about 36 images were applied, comprising of cloud-free scenes

and or less than 15% cloud cover scenes from 2010 to 2021. The image scenes were located between path/row numbers 129/50 and 129/51. These images were used to gather reflectance information from a single pixel, which provides the current field salinity. The Region of Interest (ROI) feature in ENVI was used to apply "ground truth" from eighteen salinity stations in order to detect samples from these imaginary data and organize them for producing models along with images for mapping salinity incursion intended for the full research area.

In order to normalize satellite images, the radiometric correction was primarily created to account for factors such sensor degradation, earth-sun distance variation, incidence angle, view angle, and data collection time. Later, to improve the cloudy images, a Function of mask (F-mask) technique was used to recognize clouds and cloud shadows. The completed reflectance-image, which was set up as inputs, was concentrated on the water region and clear of clouds and cloud shadows. The spectral reflectance varies depending on the object, but the range should be scaled 0–1. (Peddle et al., 2001). The spectral reflectance of water is often quite low. Between 400 and 850 nm, salty water had a small wavelength reflectance that ranged from 0.01 to 0.14. (Xiong et al., 2012).

3.2.2 Detecting Water Area from Landsat-8

Water body of the area is extracted by Normalised Difference Water Index (NDWI). The NDWI index was proposed by McFeeters in 1996 (McFeeters, 1996). Its primary application is to detect and monitor slight changes in water content of the water bodies. Taking advantage of the NIR (near-infrared) and GREEN (visible green) spectral bands, the NDWI can enhance the water bodies in a satellite image. The resulted water body is again checked with google map for cross-checking since NDWI is sensitive to build structures, which can lead to overestimation of water bodies.

3.2.3 Water Quality Time Series Data

In this study, 12-year time series data, from 2010 to 2021, of measured water quality parameters, especially TDS and EC values of the BPK River, provided by the Pollution Control Department was used. The data is comprised of 18 sampling

stations, where water quality parameters are measured quarterly each year, i.e., February, May, August, and November.

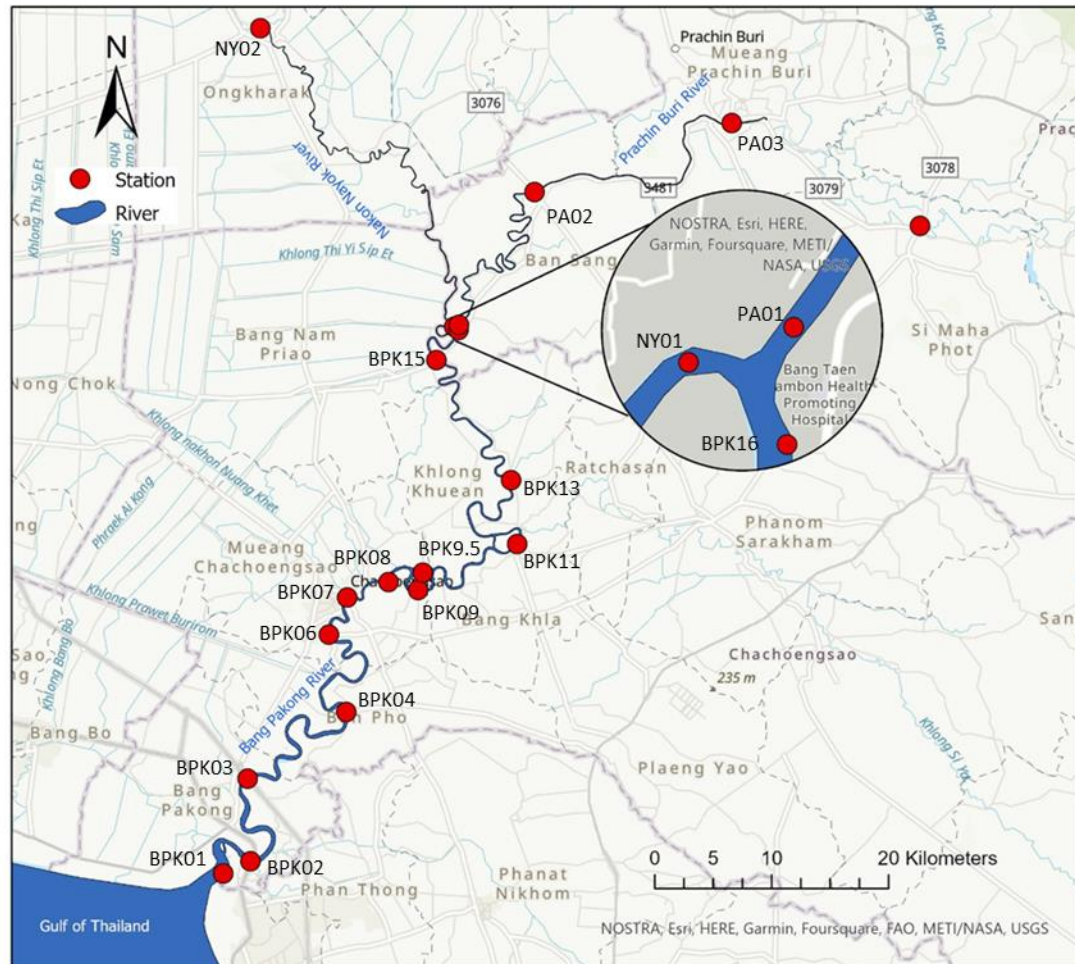


Figure 3.1 Location Map of Bang Pakong River, including upstream part: Nakhon Nayok River and Prachin Buri River. The junction in the circle represents the confluence of Nakhon Nayok and Prachin Buri Rivers.

3.3 Model Development for Remote Sensing

To evaluate efficient band compositions, seven bands are employed in the present study, and bands are selected via multi-linear regression in terms of high R^2 and lower p-value. Decision Trees (DT), Random Forest (RF), Multilinear Regression (MLR), and Artificial Neural Network (ANN) were employed to create the association between salinity and reflectance from Landsat-8 by working in R software. The best model was applied to calculate salinity intrusion for the whole

study area by using R software and ArcGIS. Meanwhile, correlation and regression analysis were used to find out the importance of climate parameters and water level on salinity—EC and TDS—of the BPK River. Figure 3.2 summarizes the flow of the research.

3.3.1 Preparation of Reflectance Wavelength - Bands Data

Reflectance wavelength data from seven bands were chosen because they were thought to study the relationship between salinity observation and both single bands and multiple bands. These relations were analyzed using the MLR. The p-value and R-square (R^2) were evaluated as parameters to determine which were effective input bands to use when using the best statistical model.

3.3.2 Salinity Modelling with Reflectance Wavelength

The original samples were analyzed using three models: ML, DTs, and RF. 282 samples from a real data set were prepared as the input for these models, which were then randomly divided into 70:15:15 for training, testing, and validation.

3.3.3 Resampling by Bootstrap Data

Bootstrapping entails repeatedly sampling at random from the data set and attempting to approximate each resampled data set's implicit effect (Preacher and Hayes, 2008). The independent and dependent variables are kept constant in pairs at the same time (MacKinnon, 2007). The bootstrap function in R was used to perform a total of 282 samples for resampling twice and four times, and it was divided into 70:15:15 samples for training, testing, and validation.

3.3.4 Salinity Modelling with Reflectance Wavelength Using Bootstrap Data

To prepare the resampling data as the response for developing salinity utilizing MLR, DTs, ANN, and RF, it was divided up 70% for training, 15% testing, and 15% validation. These models were used to determine the most effective salinity model established on reflectance, from the Landsat-8 data as well as to determine how the sample size affected how effectively the salinity model might be improved.

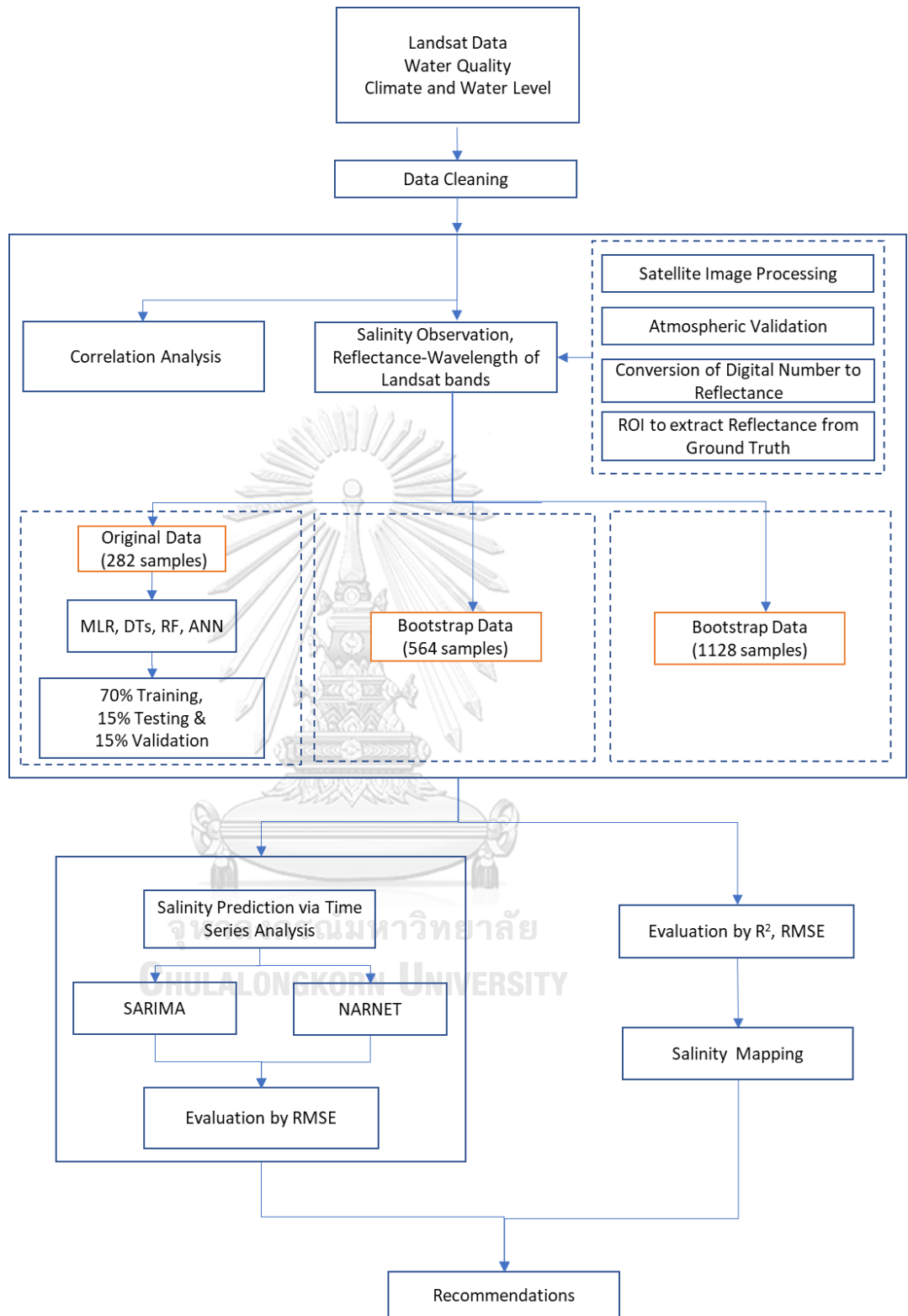


Figure 3.2 Methodology Flow Chart

- Multiple Linear Regression

For analyzing the relationship between multiple independent factors and a single dependent variable, the MLR is a highly flexible mean. R software is used to do the analysis.

- Decision Trees

The DTs's foundation was splits and nodes. In each split situation, a variable and its level are selected with the goal of making each child node as clear as possible at that level. Recursive partitioning was used in R software to accommodate the DTs (Rpart).

- Random Forest

A huge number of regression trees are combined via the ensemble-learning technique known as the RF algorithm. Two factors need to be changed within the integrated package of "randomForest" in the R application. Since RF trees are resistant to overfitting, a total of 1000 trees and a default value of one third of the total number of input variables per node are used for this study in line with the findings of (Wang, et al., 2016).

- Neural network

The ANN is typically a fantastic fit for identifying complex patterns, despite the fact that the resulting black box network is quite challenging to understand (Valbuena, Maltamo and Packalen, 2016). The inputs, the hidden layer, and the outputs are the three basic components of a neural network. To forecast a nonlinear situation, the ANN uses multi-layer connections with the weight and activation function (Niu et al., 2019a). The feed-forward neural networks with 10 hidden layers were used in this investigation.

3.3.5 Data Validation

The suggested MLR, DT, RF, and ANN models are validated using 85% of the data (70% training and 15% testing), while the remaining 15% are used for model validation. Two metrics—the coefficient of determination (R^2) and the root mean square error—are used to judge the accuracy of the various forecasts (RMSE). The goodness of the fit is gauged by R^2 (Eq. 5):

$$R^2 = 1 - \frac{RSS}{TSS} \quad (5)$$

where R^2 is coefficient of determination; RSS is sum of squares of residuals, while TSS is total sum of squares. RMSE indicates the magnitude of the error (Eq.6).

$$RMSE = \sqrt{\frac{\sum_{i=1}^N (x_i - \hat{x}_i)^2}{N}} \quad (6)$$

where RMSE is root-mean square error; i is variable i ; N is number of non-missing data points; x_i is actual observation time series; \hat{x}_i is estimated time series.

3.4 Time Series Prediction on Salinity

3.4.1 SARIMA and NARNET Models

The salinity value is processed with R software for Seasonal auto-regressive integrated moving average (SARIMA) while MATLAB software for Non-linear Auto Regressive Neural Network (NARNET) Analysis to produce the future salinity concentrations of the BPK River area.

Firstly, for the SARIMA model, quarterly EC time series data (2010-2021) is divided into testing and training; training is from 2010 to 2019 while testing is from 2020 to 2021 respectively. Each EC time series data from stations of the main BPK river are plotted, and possible outliers are searched using the 'ts' function in R. Plus, the normal distribution of the data is checked to represent real-valued random variables whose distributions are not known. After the screening of the data, the variance of the time series data is stabilized by the Box-Cox transformation, and the nature of the trend, in this case, the seasonality of the data is observed. In order to execute the time series analysis, the conversion of non-stationary to stationary is done through seasonal and regular differencing. The assumption for the Augmented Dickey-Fuller Test (ADF) on the original time series is as the following: the EC series is non-stationary (H_0) while the EC series is stationary (H_1), in which the p-value of the ADF result is greater than 0.05, it fails to reject the H_0 ; so, the EC series is non-stationary. However, in this study, the values of ACF tests are less than the p-value of 0.05 where secondary differencing is not necessary.

3.4.2 Data Evaluation

To evaluate the proposed SARIMA and NARNET models, various forecasts are assessed using the root mean square error (RMSE). RMSE indicates the magnitude of the error, applying (Eq.6).

3.5 Salinity Mapping

Salinity data are delineated with the framework from Table 3.1 for salinity assessment consisting of two methods (Wassmann *et al.*, 2019). Method 1 resulted in highly resolved map for a low-water year (salinity) in the highest salinity of a year. Method 2 presents the spatial and temporal dynamics of salinity through continuous mapping of the critical period, i.e., February for the BPK.

Table 3.1 Framework for defining and mapping salinity

Method	Mapping attributes of salinity
1) Peak salinity maps	Maximum salinity of year
2) Time-sequenced maps	Salinity year as time-sequenced maps

CHAPTER 4

RESULTS AND DISCUSSIONS

4.1 Assessing Salinity via Remote Sensing and GIS Methods

4.1.1 Relationship between the reflectance and salinity

The composite Landsat 8 spectral bands, including Band 1's ultra-blue (coastal) wavelength, Band 2's blue, Band 3's green, Band 4's red, Band 5's near infrared (NIR), Band 6's shortwave infrared (SWIR-1) wavelength, and Band 7's shortwave infrared (SWIR-2) wavelength, offered highly effective salinity model prediction significance (Figure 4.1). With a p-value of 0.0193, the combination of Bands 2, 3, and 4 also indicates the highest importance, surpassing that of Bands 1 through 7 (p-value: 0.1282), Band 23 (p-value: 0.02879), and Band 321. (p-value: 0.04186). The individual bands 2 and 3 have high p-values, but compared to the composite bands, it is unlikely that using single bands will be as effective. As a result, four bands—namely, Bands 2, 3, 4, and 7—are chosen as the salinity model's input variables. In contrast to Band 234 (Figure 4.3), which has mixing color, Band 247 (Figure 4.2) exhibits a more constant and obvious pattern across the whole research region.

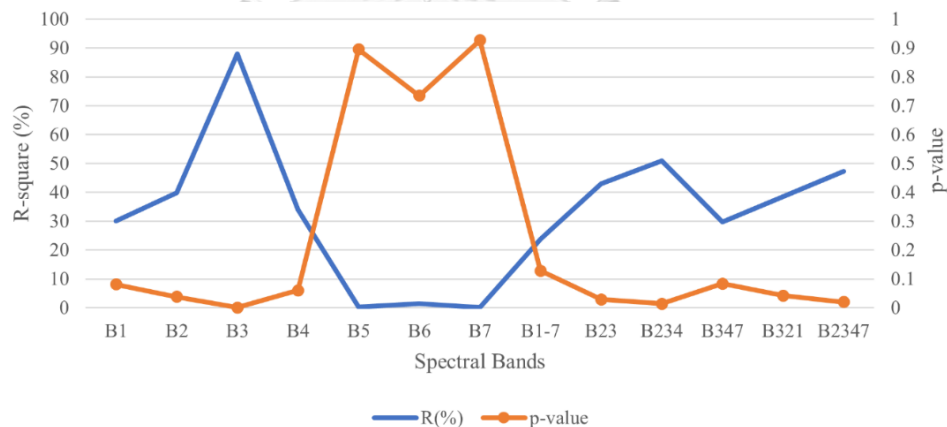


Figure 4.1 Multiple linear analysis of the relationship between salinity and composite bands. R-squared is indicated with blue line, while p-value is shown with orange line.

The accuracy of the salinity map depends on the selection of Landsat bands for the model, thus it's important to pay attention to both the R-square and RMSE of the model as well as the composite wavelength data used as inputs for salinity of the entire area of interest. On the other hand, if attempts are made to use more possible

predictor variables, using more input variables may result in fitting that quickly becomes computationally unfeasible (Messner, Mayr and Zeileis, 2017). As a result, the salinity map's ability to predict the future depends on the right choice of bands and band composition.

A function of remotely sensed color bands can be used to determine the river's salinity (Erin A. Urquhart et al., 2012). This study discovers that the reflectance wavelengths of bands 2, 3, 4, and 7 are crucial for detecting salinity, and the band selection findings are consistent with those of (Nguyen et al., 2018). Band 1 to 5 of Landsat 5 TM was substantially associated with salinity in other investigations, in particular (Wang and Xu, 2008). The most closely similar band for salinity, however, was discovered to be TM band 3. (Wang and Xu, 2008). According to Urquhart et al. (2012), the reflectance wavelengths of MODIS at 443 nm, 488 nm, and 667 nm and those of Landsat 8 OLI at bands 1 to 4 were related to salinity (Jun Zhao, Temimi and Ghedira, 2017).

4.1.2 Salinity Modelling with Original Data

The Multilinear Regression (MLR) model gives a fairly good R^2 and RMSE of 39.61% and 12.41 in training, 34.82% and 13.75 in testing and 54.73% and 10.69 in validation respectively (Figure 4.4). The predicted salinity (dS/m) from MLR ranges from around 0 - 39.61 in training, and the range is similar in testing and validation. The Decision Tree (DT) model shows a moderately high R^2 and low RMSE of 70.15% and 8.65 in training, indicating moderate correlation, however, R^2 and RMSE values become lower as 33.54% and 13.72 in testing and 30.65% and 14.18 in validation parts (Figure 4.4). The predicted salinity (dS/m) from DT ranges from around 1.7 - 47.22 in training but 0.8 - 27.27 in testing and validation correspondingly. In terms of p-values, both models generate p-value lower than 2.2×10^{-16} , in contrast, DT outperforms MLR as it has higher R^2 and RMSE.

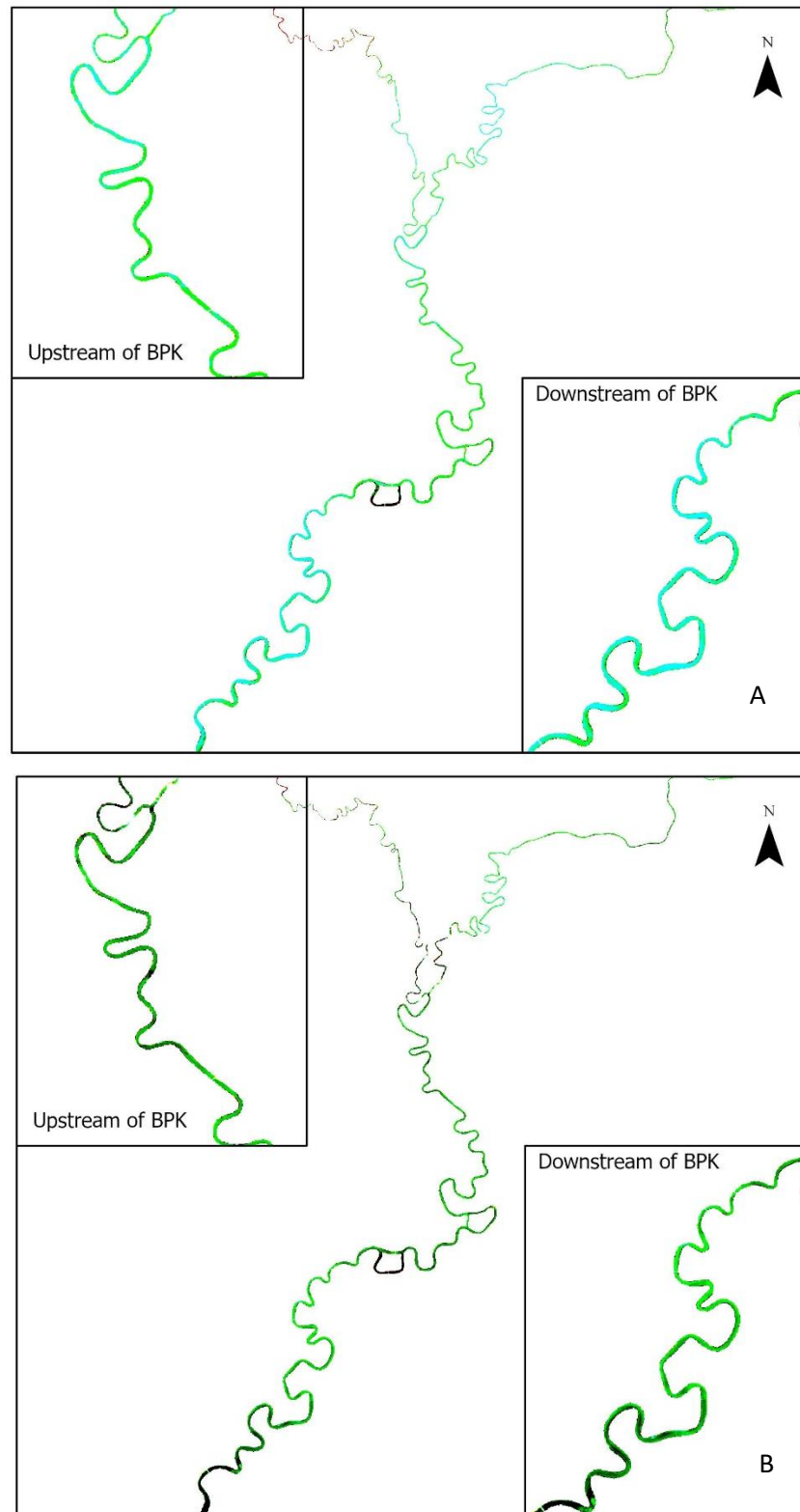


Figure 4.2 Composite band 247 on (A) February 2nd, 2020 and (B) February 5th, 2021

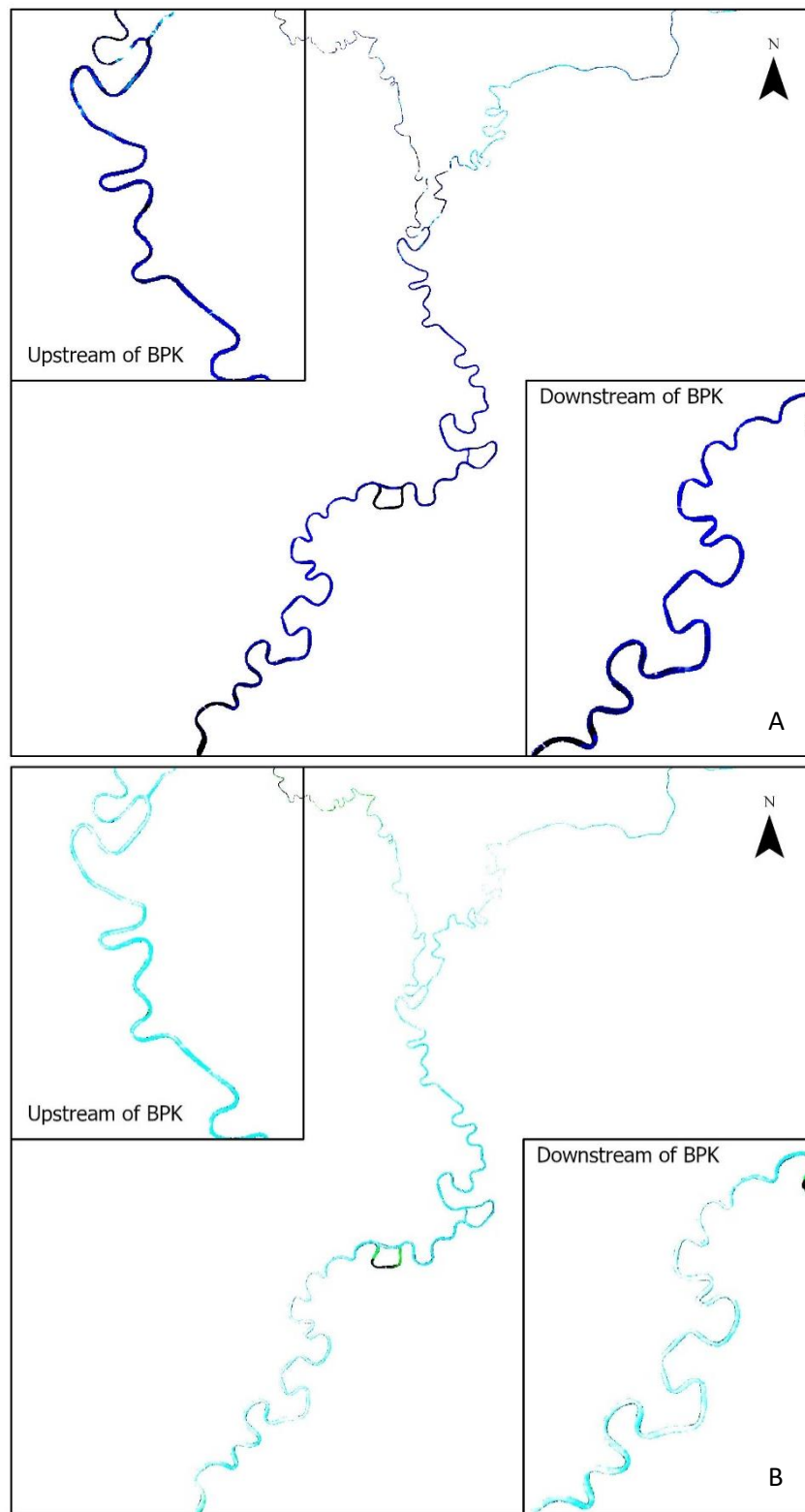


Figure 4.3 Composite band 234 on (A) February 2nd 2020, and (B) February 5th, 2021

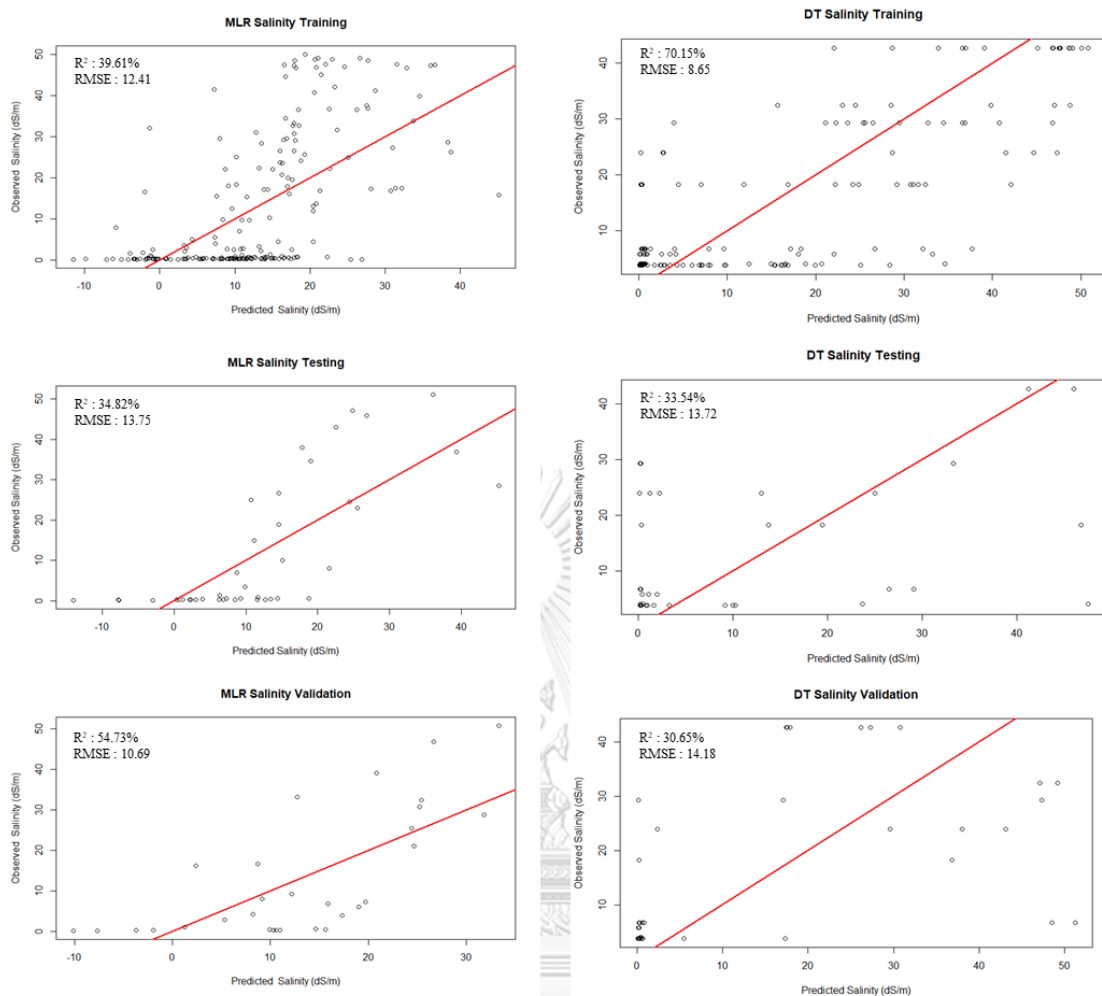


Figure 4.4 Regression of MLR and DT using the original data as 70% training, 15% testing and 15% validation

Regarding the Random Forest (RF) model, the highest R^2 of 90.57% is observed among the training part of MLR, DT and RF, along with moderately high R^2 : 53.66 % in testing and 55.08% in validation (Figure 4.5). In addition, each RMSE value varies as 11.17, 11.89 and 12.15 in training, testing and validation, i.e., having lower values than DT and MLR. On top of that, p-values of RF has a strong significant figure of less than 2.2×10^{-16} . In addition, the lower limit of the predicted salinity is 0.39 (dS/m) while the upper limit is 44.60 (dS/m) in training part. A similar range of 0.86 – 41.78 (dS/m) is learned in testing and 0.62 – 37.97 (dS/m) in validation.

The final model, Artificial Neural Network (ANN), trained by Levenberg-Marquardt algorithm with 10 hidden layers, reveals a moderately good R^2 values: 73.29% in training and 78.63% in testing with each RMSE of 11.33 and 12.46 (Figure 4.6). However, R^2 of validation makes only 58.25% with a slightly high RMSE of 13.28. In conclusion, after comparing R^2 and RMSE of four models, RF generates the best evaluation results using the original data.

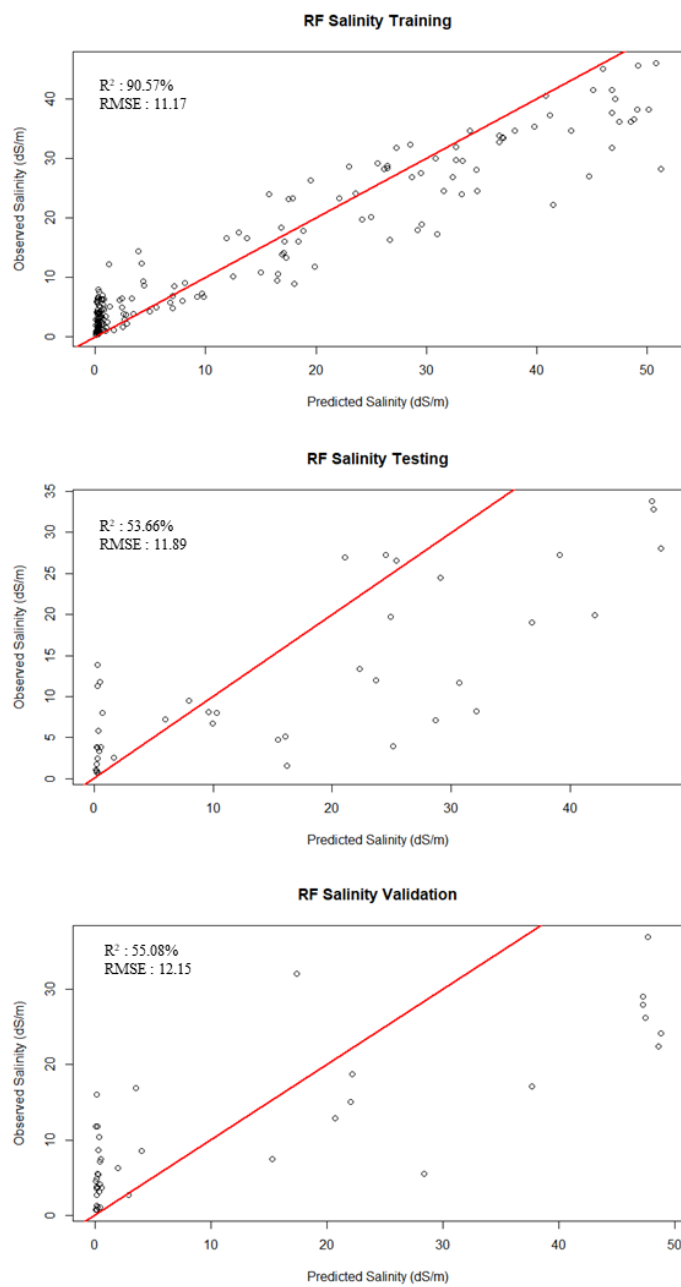


Figure 4.5 Regression of RF using the original data

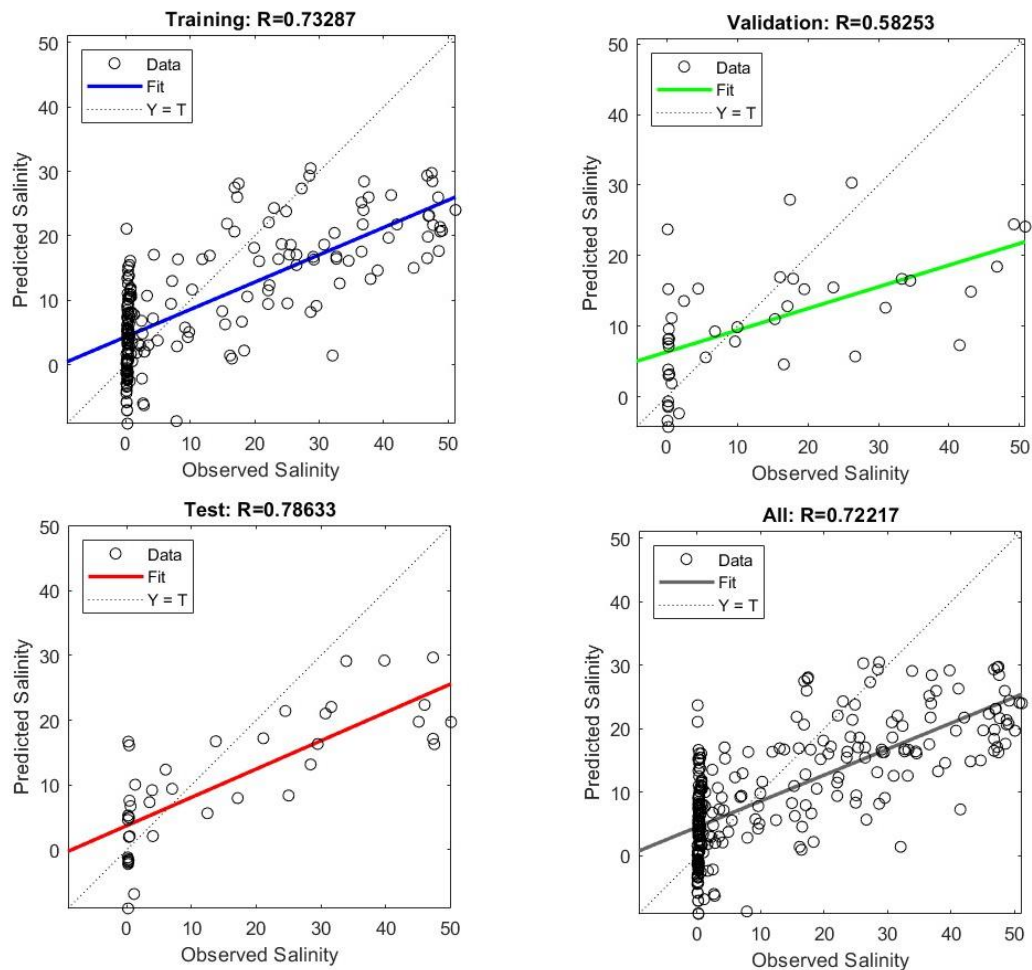


Figure 4.6 Regression of ANN using the original data

Selection of a suitable model critically affects the accuracy of the prediction and is placed the same rank of importance with variables and more significant than sample size (Fassnacht *et al.*, 2014). The MLR method undoubtedly showed the model structure, however the linear regression may lack of predicting ability for a high confidence level in the case of complex relationships between variables. In addition, the DT model proved a good potential for prediction with moderately high evaluation results in training, nonetheless, the resultant parameters are not strong enough in testing and validation. The ANN model appears a good correlation among the reflectance and the salinity, but the concern of ANN is the changing structure of the model in every single setup and rerun. To overcome this challenge, the number of hidden layers, running times for each single setup along with the training method need to be considered. In this case, the hidden layer is set up with 10 layers which is the

optimal value as the performance the model decreases with a smaller layer number. Meanwhile in terms of training method, Levenberg-Marquardt algorithm gives a fast-running speed while Bayesian Regularization algorithm can generalize well but it takes time. Thus, the ANN model is unlikely to be useful for the prediction (Niu *et al.*, 2019b).

Meanwhile, the RF model is a method of choice in many applications as RF can be effectively employed to complex data, including small sample size, intricate interactions and correlations and mixed type predictors (Epifanio, 2017b). Moreover, the RF model reveals the highest prediction capability compared with MLR and DT models (Chen *et al.*, 2017; P. T. B. Nguyen *et al.*, 2018). Accordingly, the outcome of the RF model is the best for the Salinity prediction as the other models have limitations.

4.1.3 Salinity Modelling with Bootstrap Data

The original sample size of 282 observations is used to generate two bootstrap data, comprising of 564 and 1128 observations, i.e., two and four times of the original data. All the four models, namely, MLR, DT, RF and ANN are applied with the bootstrapped data (Figure 4.7). Among the four models, R^2 and RMSE of MLR don't improve significantly but remains around 34 – 37% and 12 – 13 in training, and testing using bootstrap data, apart from validation that has slightly higher R^2 of 44% while RMSE of validation shares the similar values. Thus, bootstrapping in MLR results a small improvement, however it doesn't support considerable results to choose MLR. It is because MLR model has a simple structure and less dimensions than other models, especially when the relationship between variables are complex, this limits MLR to predict with a confidence. The DT reveals better correlation for all three parts—training, testing and validation—compared with MLR using the bootstrap data. R^2 of DT, at 1128 samples, soars to 81% in training, 70% in testing and 75% in validation, along with a decrease in RMSE around 1 unit in training, 4 units in testing, and 5 units in validation. Nonetheless, RMSE of DT is comparatively high, causing it less possible to make useful predictions, even though, substantial improvements in R^2 .

The ANN model generates good correlation not only in R^2 but also in RMSE in both 564 and 1128 bootstrapped samples. R^2 in training part enhances to 86% in 564 samples and 88% in 1128 samples with a gradual drop in RMSE of 8.4 and 7.4 respectively. A similar improvement trend can be found in testing and validation parts of ANN. Even though, there is a potential problem of overfitting in original data using ANN, this is solved by using bootstrap data. On the other hand, the RF model can be considered as the best model in terms of modelling accuracy, based on growing sample size, i.e., from original sample of 282 samples to bootstrapped samples of 564 and 1128 samples. In particular, the training part delivers R^2 of which is almost close to 100% and substantial decrease in RMSE that is the lowest among all RMSE values of models. An analogous trend is also examined in testing and validation parts of the RF model. The result of RF is comparatively strong and valid enough to be considered as the model of choice for salinity mapping.

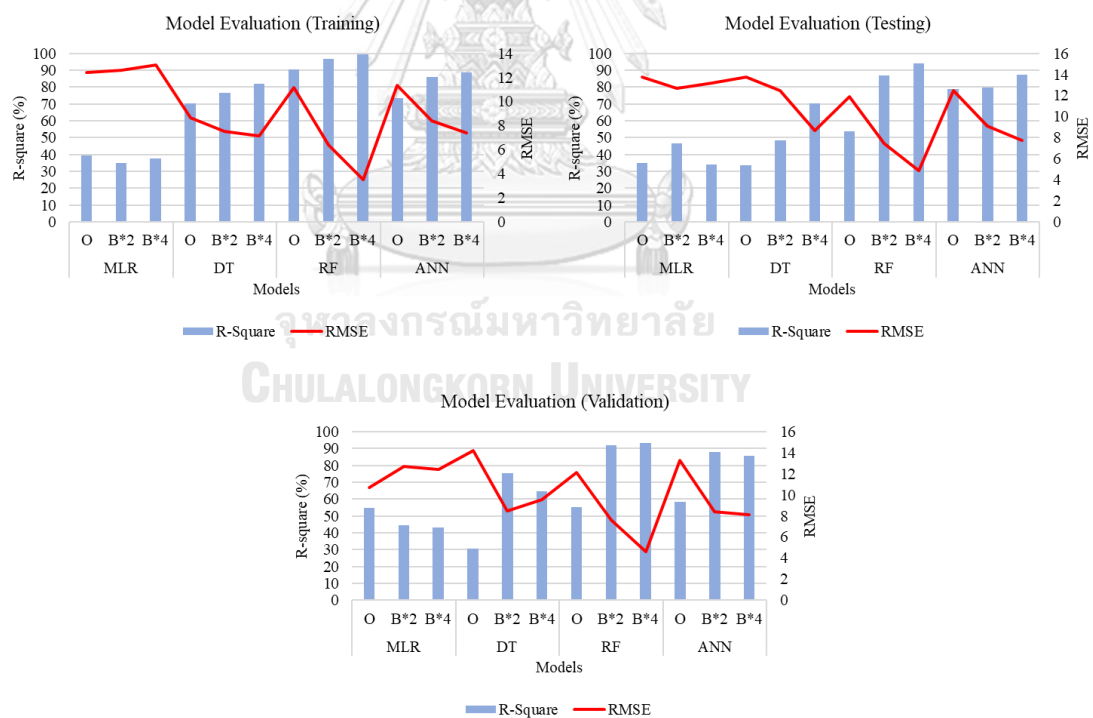


Figure 4.7 Comparison of R^2 and RMSE in training, testing and validation of models with original data (O = 282 samples) and bootstrap data (B*2 = 564 samples and B*4 = 1128 samples)

The resampling of the original data via bootstrap method is effective for the prediction ability of the models, specifically if the observations are not sufficient. Based on the results of each model, increasing the sample size drastically enhances the correlation of models—MLR, DT, RF and ANN—and overcomes the overfitting problem in using the original sample. The ANN model appears a good correlation among the reflectance and the salinity, but the concern of ANN is the changing structure of the model in every single setup and rerun. Thus, the ANN model is unlikely to be useful for the prediction (Niu et al., 2019).

The RF is observed as the best performance at the resampling of both 564 and 1128 samples in all three parts—training, testing and validation of the model. The RF describes the effective prediction of the data in a larger sample size (Fassnacht *et al.*, 2014). It is important to note the sample size of the original data is a challenge in using bootstrap method. It is because when the sample size is very small, it can lead to over repetition in the selection of data. Thus, in this case, even though the model has a great correlation, the practicality is constrained in applying salinity mapping for the whole study area. The performance of the bootstrap depends on the sample size, and it is hard to recommend a minimum sample size because varying circumstances that requires different minimum sample size (Dixon, 2001).

4.1.4 Salinity Mapping

Peak salinity maps, i.e., salinity of February which is the highest in a year, from 2018 to 2021 can be delineated according to different levels of salinity in dS/m (Figure 4.8 to 4.11). The salinity can be categorized as shown in Table 4.1, based on the FAO classification of saline water for irrigation (Rhoades, Kandiah and Mashali, 2012). Different levels of salinity are observed along the river, which can generally divided into four major areas: downstream of BPK, upstream of BPK, tributary of Nakon Nayok, and tributary of Prachin Buri. Among these four segments, the downstream part of BPK clearly show the highest salinity and exhibits the seasonality changes., in particular February has the highest salinity and November has the lowest salinity (Figure 4.14). Regarding the time-sequence maps, including upstream (Figure 4.13) and downstream (Figure 4.12) of BPK river, the annual changes in the salinity can be observed and it can be considered that, in general, the variation is more

noticeable in the downstream of the BPK river, especially to BPK9.5. The reason of increasing salinity is related to increasing sea intrusion, slow discharge of river and low lying geography of the area, which elevation is less than about 10 m, making the saline water to flow into the river (Royal Irrigation Department, 2010 and Hydro and Agro Informatics Institute HAI, 2012). Man-made factors, in this case, are discharge from dams (upper parts of the river basin) to push down saline water and water usage for agricultural activities (higher water demand than water supply) creating the pull of seawater by overconsumption for agriculture (Molle, Srijantr, and Promchote, 2009). Direct impact of salt intrusion was substantially noticeable in the main river than in the canals (Bubphamala et al, 2010).

These results are in line with a study of (Yuenyong et al., 2019) revealed that high salinity in the BPK River was reported at the river mouth, especially in the dry season, i.e., February. Bordalo et al. (2001) also observed that the average water quality index (WQI) of the BPK River was quite low and water quality declined significantly during dry period (Bordalo, Nilsumranchit and Chalermwat, 2001). Sea water salinity creeps into the basin up to Prachin Buri because of overuse of water in the dry season (Molle, Srijantr, and Promchote, 2009).

Table 4.1 Classification of saline water

Water Class	EC (dS/m)	Tds (mg/l)
Non-Saline	<0.7	< 500
Slightly Saline	0.7 - 2	500 - 1500
Moderately Saline	2 - 10	1500 - 7000
Highly Saline	10 - 25	7000 – 15000
Very Highly Saline	25 - 45	15000 - 35000
Brine	> 45	> 35000

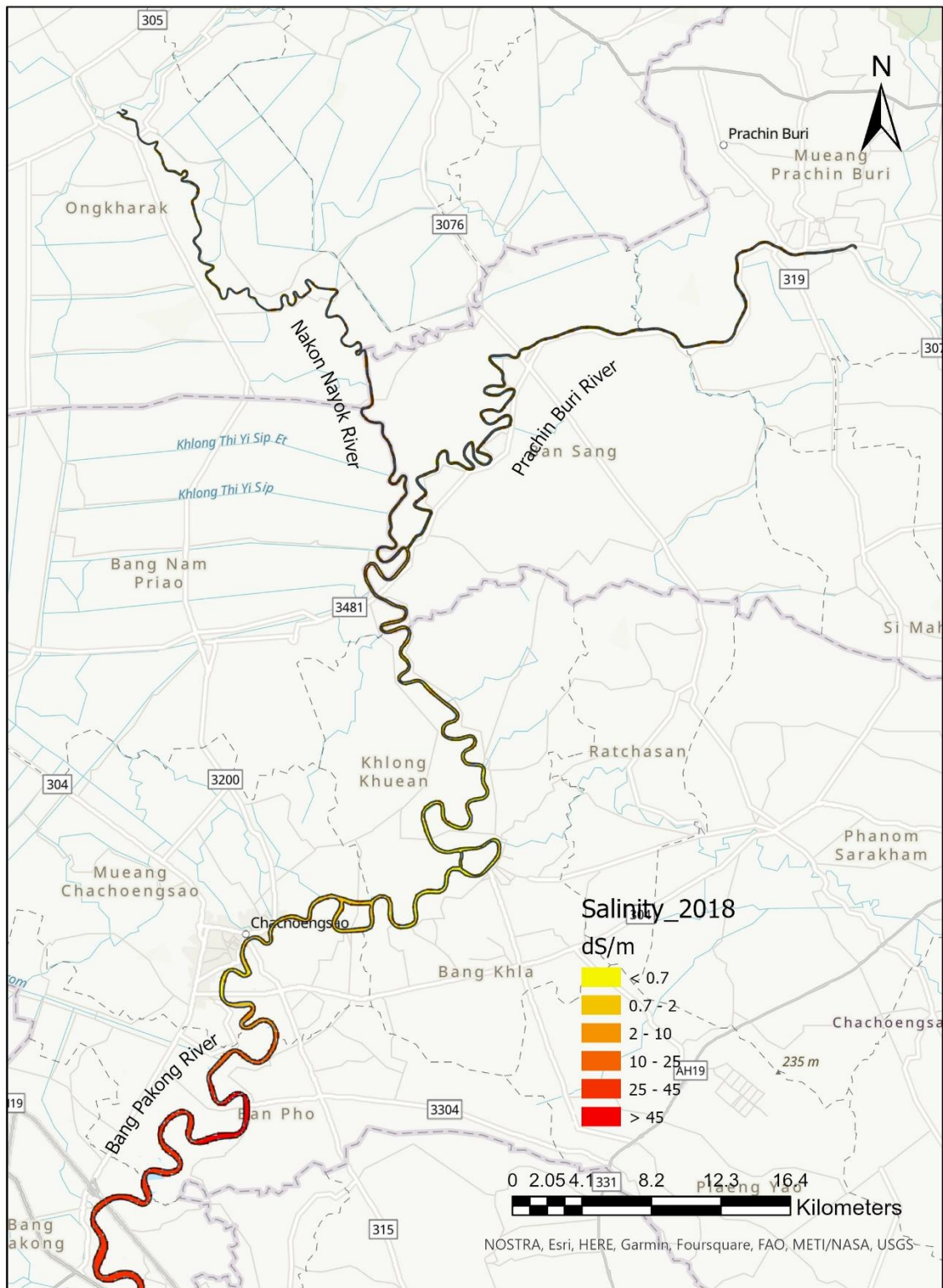


Figure 4.8 Salinity Map of BPK in February 2018

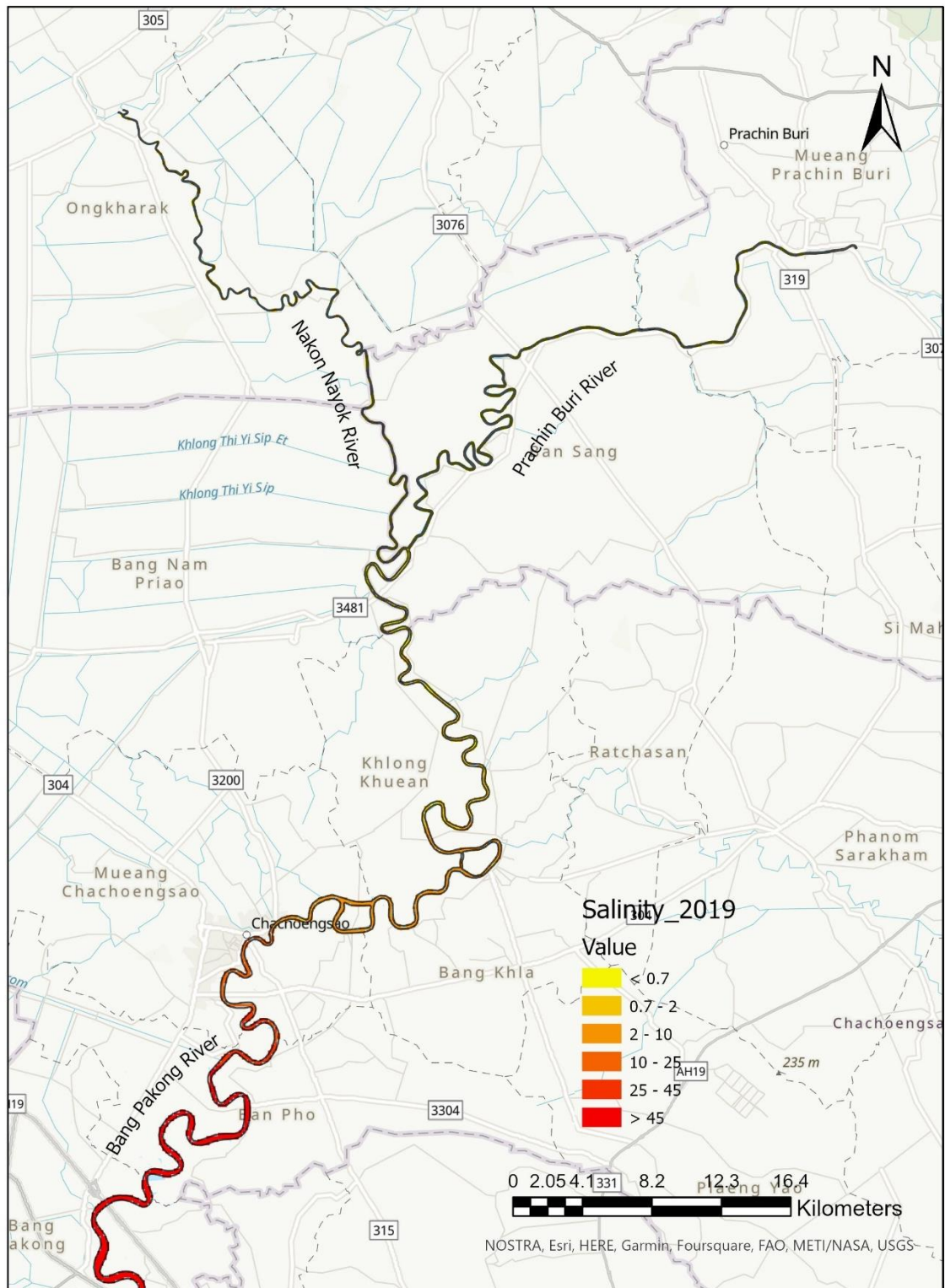


Figure 4.9 Salinity Map of BPK in February 2019

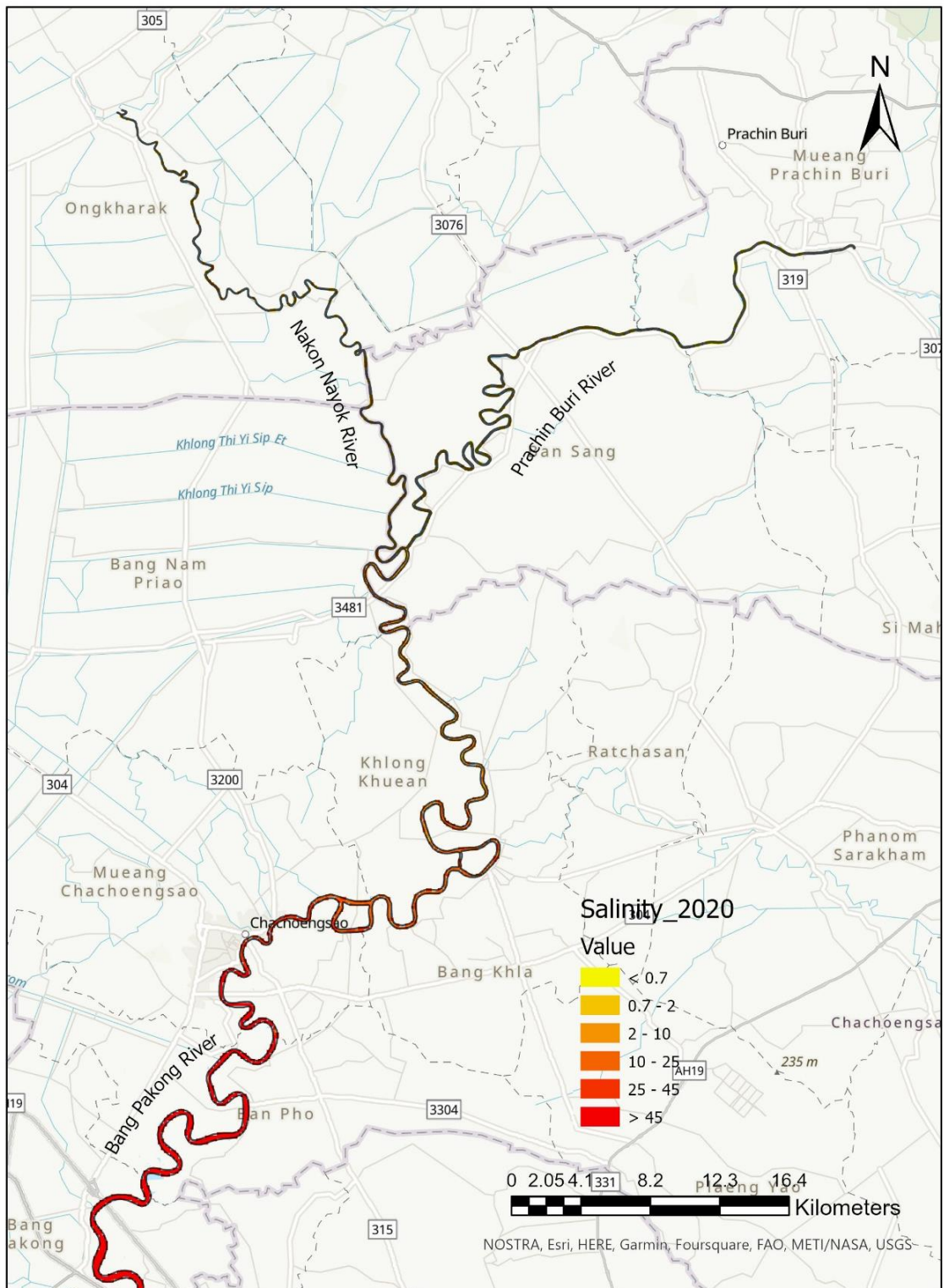


Figure 4.10 Salinity Map of BPK in February 2020

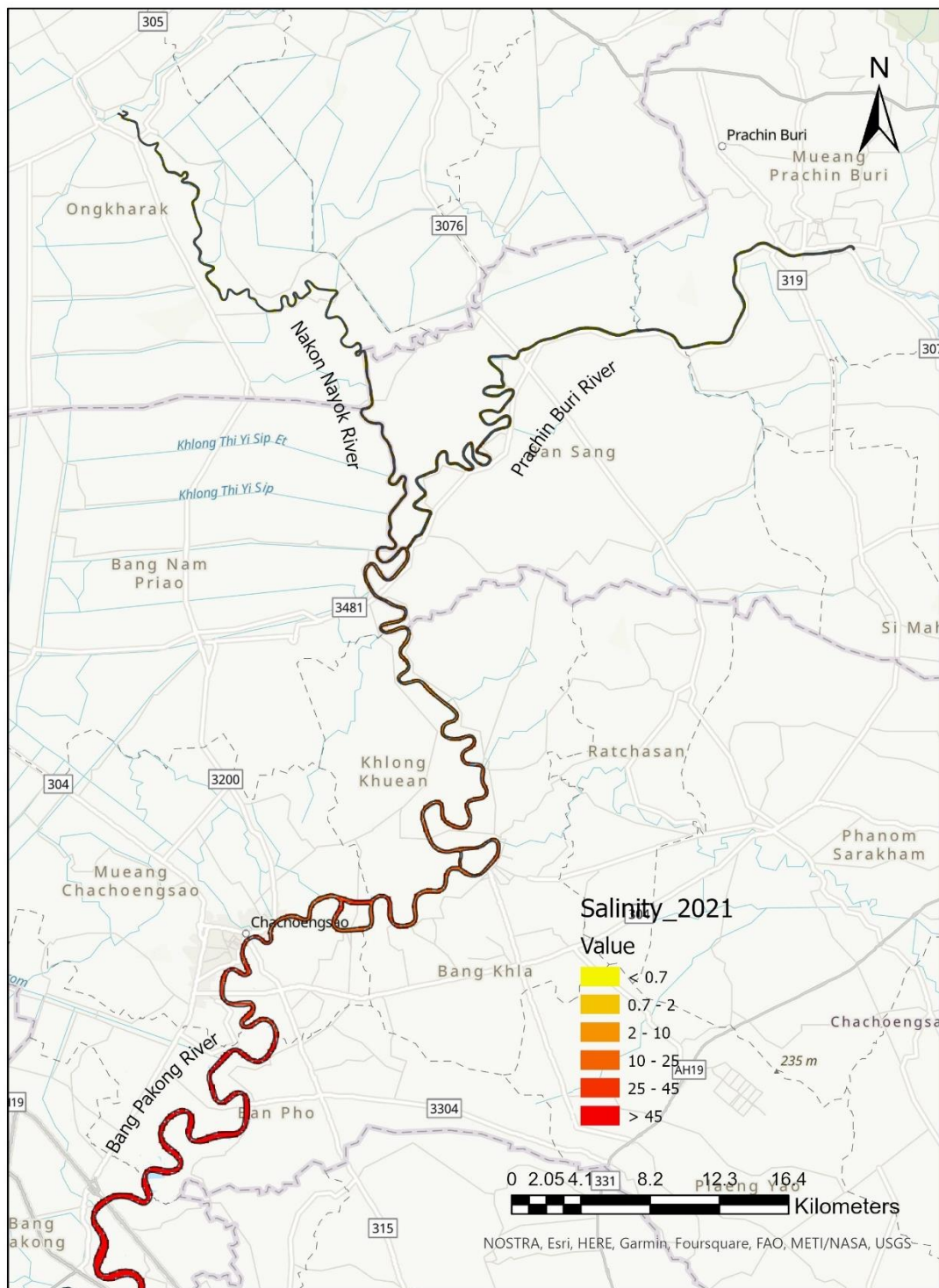


Figure 4.11 Salinity Map of BPK in February 2021

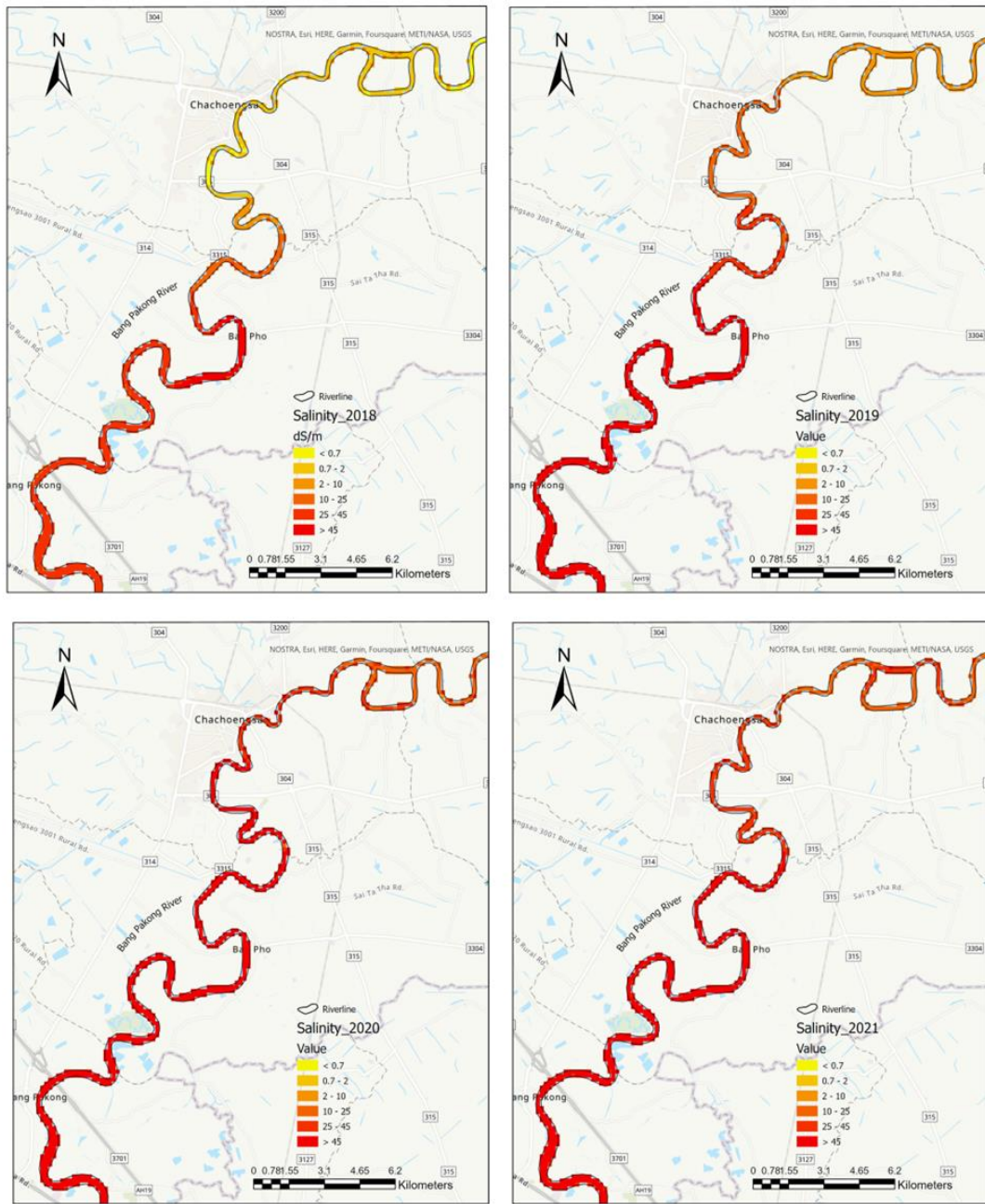


Figure 4.12 Salinity variation of BPK downstream part from 2018 to 2021

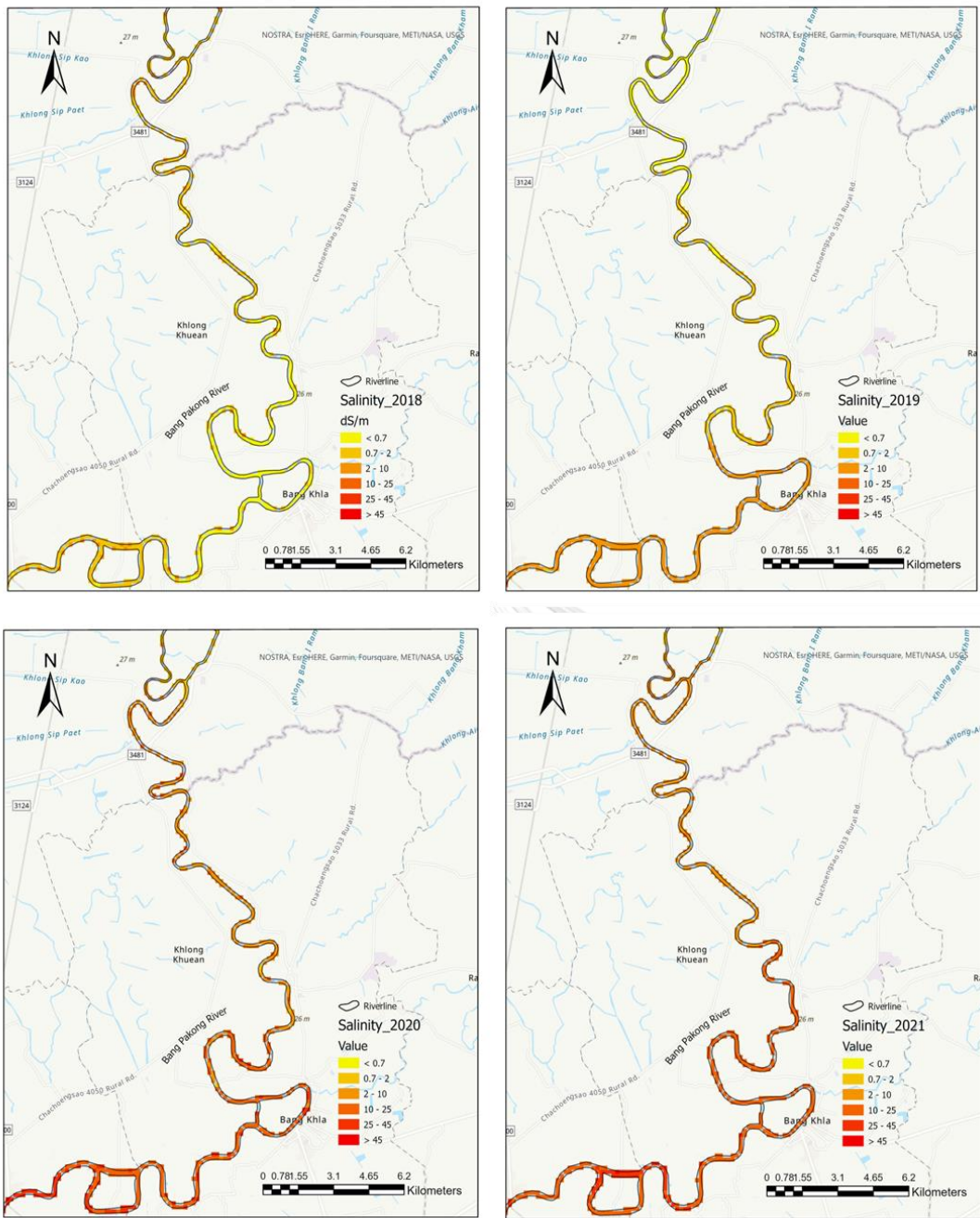


Figure 4.13 Salinity variation of BPK upstream part from 2018 to 2021

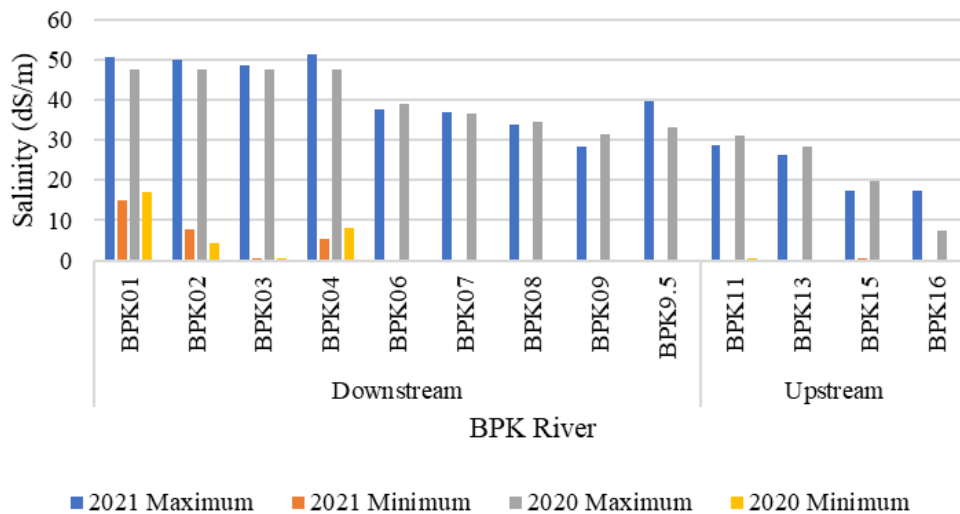


Figure 4.14 Observed maximum and minimum salinity along the main BPK river

4.2 Assessing Salinity via Time Series Methods

4.2.1 Results of SARIMA Model

Different SARIMA models are generated for different stations as the salinity values vary from one station to another. It can be generally categorized into five models—Group 1: BPK01, Group 2: BPK02 and 04, Group 3: BPK03, Group 4: BPK06 to BPK9.5 and Group 5: BPK11 to BPK16 (Annex 1). Each group shares the same model due to their geographical locations along the river. However, the results of stations: BPK01, BPK02, BPK03, BPK06 and BPK11 are selected to represent the geographical distribution of stations—upstream station: BPK11, mid-stream stations: BPK06, and downstream station: BPK01, BPK02 and BPK03—along the river.

From Total Correlation Chart: Auto-correlation Function (ACF) and Partial Correlation Function (PACF) plots (Figure 4.15), all five stations fit well with non-seasonal part of the model (p, d , and q) equals to 0 suggesting that the salinity value is associated with seasonal pattern. All the values in the ACF and PACF plot fall within the 95% confidence band (Blue-dotted line). Detailed statistics of each selected station and their representative model with the Akaike information criterion (AIC), the Bayesian information criterion (BIC), RMSE and MAE can be observed in Table 4.2.

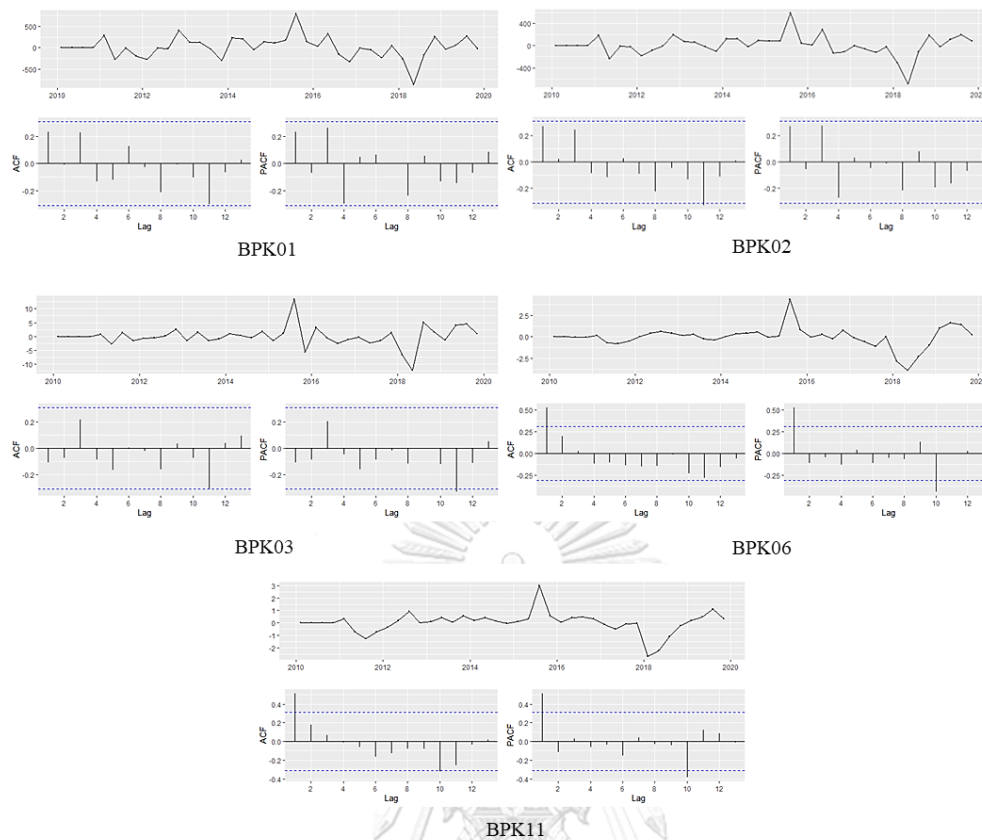


Figure 4.15 ACF and PACF plots of ARIMA models from each group, starting from BPK01 to BPK11

Table 4.2 Statistics of each selected station along the BPK River

<i>Station No</i>	<i>SARIMA Model</i> $(p,d,q)(P,D,Q)(m)$	<i>AIC</i>	<i>BIC</i>	<i>RMSE</i>	<i>MAE</i>
<i>BPK01</i>	(0,0,0)(1,1,2)[4]	525.40	533.32	10.13	7.08
<i>BPK02</i>	(0,0,0)(0,1,1)[4]	498.09	502.84	10.03	6.80
<i>BPK03</i>	(0,0,1)(0,1,1)[4]	212.18	218.52	9.42	5.69
<i>BPK06</i>	(0,0,0)(2,1,0)[4]	130.19	136.53	10.79	5.98
<i>BPK11</i>	(0,0,0)(0,1,1)[4]	106.12	110.87	7.90	4.87

4.2.2 Results of NARNET Model

Before executing the NARNET, the optimal numbers of hidden layers in the neural network are defined. Based on MSE values of three time running of a total of 10 layers, using 10 layers is the best for the analysis (Figure 4.16). Stations for NARNET can be generally categorized into three groups—Group 1: BPK01, BPK02, BPK03, and BPK04, Group 2: BPK06 to BPK9.5 and Group 3: BPK11 to BPK16. Each group are defined based on their geographical locations along the river (Annex 2). In order to compare easily with the results of the SARIMA, stations: BPK01, BPK02, BPK03, BPK06 and BPK11 are selected representing upstream, mid-stream and downstream parts of the BPK river. Table 4.3 and Figure 4.17 describes the performance of the NARNET model on the selected stations. In terms of RMSE values, higher RMSE units are observed at the downstream part while the unit gets lower in the upper part of the river.

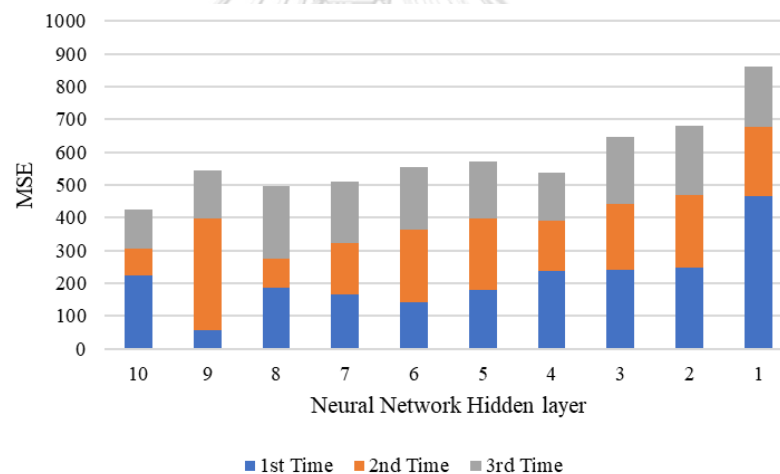


Figure 4.16 Comparison of MSE vs numbers of hidden layers

Table 4.3 NARNET model parameters of each selected station along the BPK River

<i>Station</i>	<i>MSE</i>	<i>RMSE</i>	<i>R²</i>
<i>BPK01</i>	190.7485	13.81117	66.87
<i>BPK02</i>	177.161	13.31018	71.88
<i>BPK03</i>	131.3151	11.45928	81.92
<i>BPK06</i>	165.0492	12.84715	62.22
<i>BPK11</i>	92.79349958	9.632938	66.14

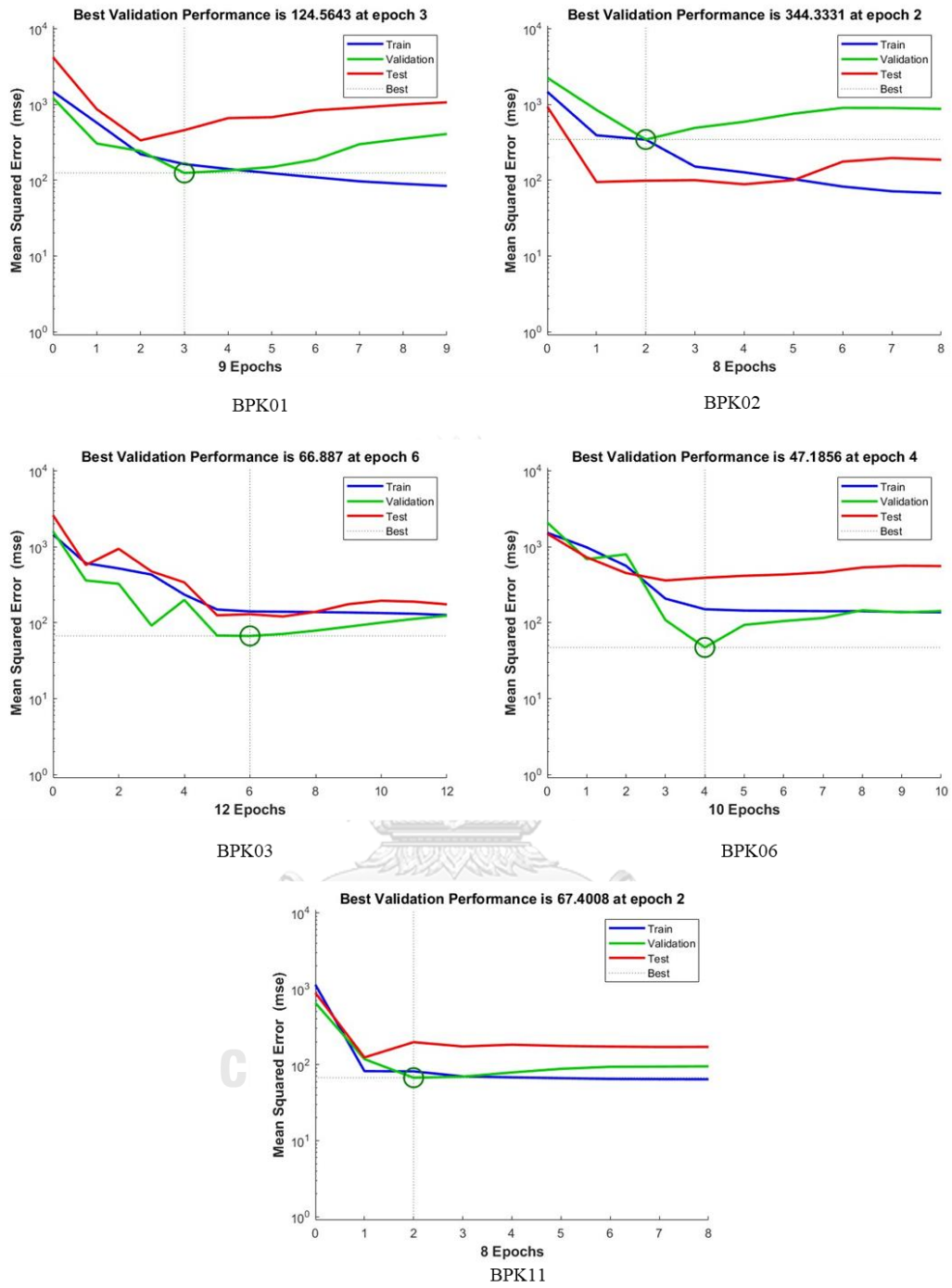


Figure 4.17 Performance plot of NARNET at selected stations

4.2.3 Discussions on Time Series Models

Based on the forecasted results (Figure 4.18 and 4.19), the salinity of the BPK river has a similar pattern every year, high salinity is observed especially during quarters of February and May. These results are consistent with (Yuenyong et al., 2019) and it revealed that high salinity in the BPK River was reported at the river mouth, especially in the dry season. In addition, in comparing the salinity of both SARIMA and NARNET models, SARIMA models yield lower RMSE units from 9 – 10 while 11 – 13 in the NARNET, in particular at the downstream part—BPK01 to BPK03—of the BPK river. Similarly, in the upper and mid-stream of the river, NARNET shows higher RMSE of 12.84 at BPK06 and 9.6 at BPK11 while under the SARIMA, RMSE are 10.79 and 7.9. Thus, SARIMA outperforms NARNET in the upper, mid, and downstream parts of the river. Stations BPK06 and BPK11 do not have a good performance, i.e., under-forecasted salinity compared with monitored values as the rate of change (from 2018-2021) in these stations are as high as 9% and 7% respectively (Figure 4.18), however, stations BPK01, BPK02 and BPK03 have close estimates, contrasted with monitored data, along with their overall lower rate of change of less than 5%.

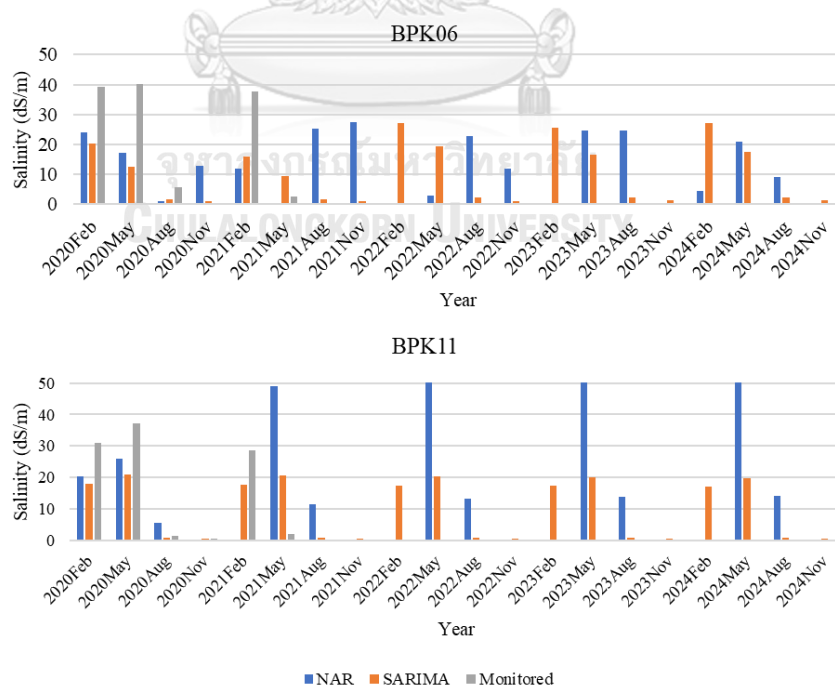


Figure 4.18 Comparison of salinity values of SARIMA, NARNET(NAR) and measured at the mid and upstream part of the BPK river.

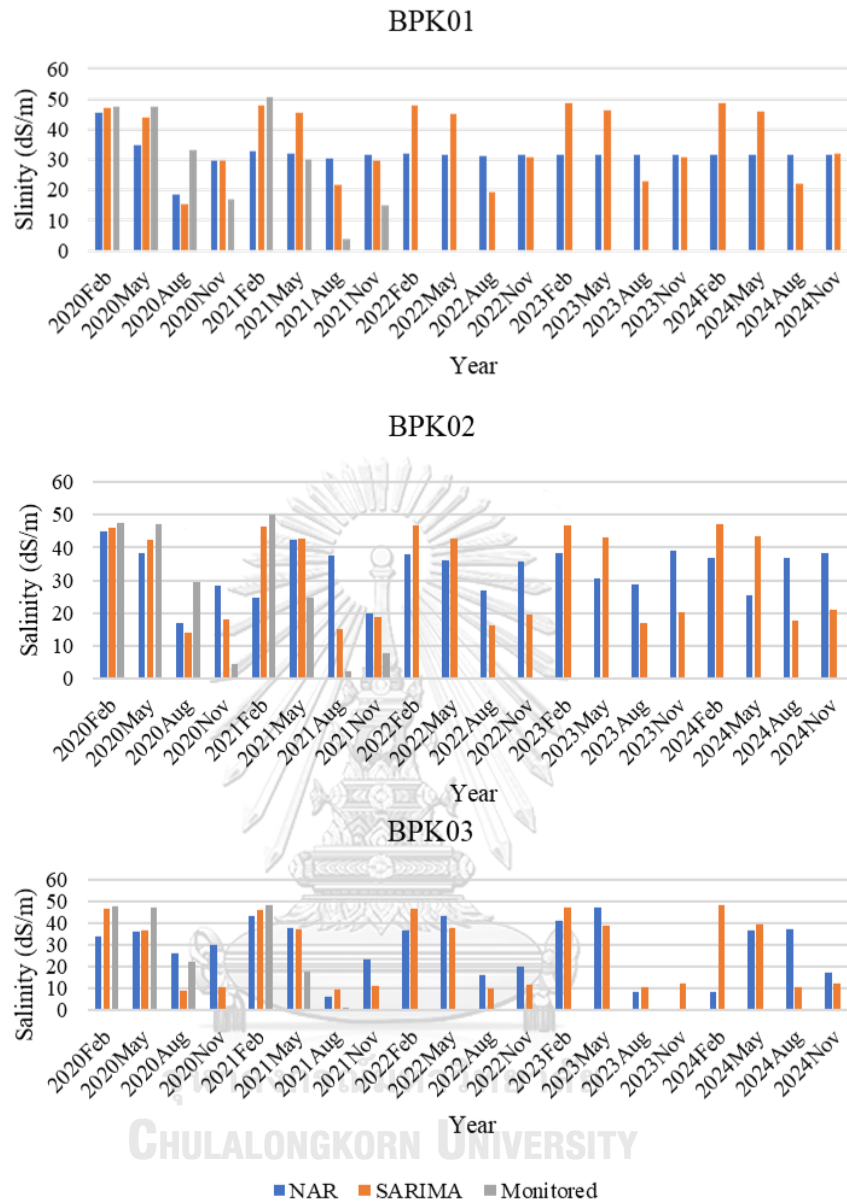


Figure 4.19 Comparison of salinity values of SARIMA, NARNET(NAR) and measured at the downstream part of the BPK river

It is because the SARIMA model can grasp the historical information by (1) seasonal and regular differences to achieve stationarity, (2) AR to take into account the past values, and (3) MA to take into account the current and previous residual series. Thus, the SARIMA model has advantages in its well-known statistical properties and effective modelling process.

4.3. Investigation of Climate and Water-related Factors on Salinity

In order to find out the relationship between each variable, correlation matrix (Table 4.4), and multilinear regression (Table 4.5) are conducted. Water level, air temperature and precipitation data are quarterly average data, representing the provincial coverage while water temperature, EC and TDS are collected along the local stations with the similar quarterly timeframe. When regressing EC with other water and climate variables, it generates 12.97 % of R^2 with a p-value of 9.32×10^{-52} . Meanwhile, the R^2 of TDS vs other variables give 17.62 % and p-value of 5.86×10^{-25} .

Table 4.4 Correlation matrix of water quality and climate parameters

	Water Temperature (°C)	Air Temperature (°C)	Precipitation (mm)	Water level (m)	EC (dS/m)	TDS (mg/l)
Water Temperature (°C)	1					
Air Temperature (°C)	0.78253734	1				
Precipitation (mm)	0.430258701	0.37346	1			
Water level (m)	-0.195632631	-0.21644	-0.35645	1		
EC (dS/m)	0.106000429	0.226412	-0.17072	0.016189	1	
TDS (mg/l)	0.145718605	0.298386	-0.14949	-0.02801	0.730931	1

Table 4.5 Regression summary of TDS and EC vs climate and water-related variables

Regression	R Square	Significance F
TDS	0.419808	5.86E-25
EC	0.360212	9.32E-52

Variables	EC P-value	TDS P-value
Water Temperature (°C)	0.188	0.042
Air Temperature (°C)	1.62E-10	3.22671E-16
Precipitation (mm)	8.42E-11	4.8375E-12
Water Level (m)	0.665	0.188

From Table (4.4), it can be observed that precipitation and the salinity have the inverse relationship as input of rainwater dilutes the salts in river water, thus

decreasing the salt concentration. Regarding precipitation and salinity correlation, in terms of EC: Pearson Correlation is -0.170 (p-value < 0.05) and TDS: Pearson Correlation is -0.149 (p-value < 0.05). In addition, temperatures of both water and atmosphere have fair correlations: 0.22 for air (p-value < 0.05) and 0.1 for water (p-value < 0.05) with EC and 0.29 for air (p-value < 0.05) and 0.14 for water (p-value < 0.05). However, the water level has no relationship with the salinity, in which Pearson correlation value is 0.01 with EC and -0.02 with TDS respectively, i.e., water level is not statistically significant.

Hayashi, 2004 examined the EC-temperature relation of natural waters having vastly different compositions and salinities and concluded EC-temperature relation was slightly nonlinear in a temperature range 0-30 °C (Hayashi, 2004). Ouma, et al, 2020 proved that Pearson correlation coefficient of temperature and EC is positive with 0.28 (Ouma, Okuku and Njau, 2020). (Katsaros and Buettner, 1969) Katsaros and Buettner, 1969 also proved that falling rain changes water surface conditions, because of its different salinity, different temperature, and its momentum (Katsaros and Buettner, 1969). Weijs, et al, 2013 suggested that stream discharge is more relevant parameter in investigating the relation with salinity, compared to stream level, which can be affected by the streambed due to sedimentation (Weijs, Mutzner and Parlange, 2013). For the case of BPK, the dominant factors are high water demand (overconsumption for agricultural uses) and low discharge. Royal Irrigation Department (2010) and Hydro and Agro Informatics Institute (HAI) (2012) stated that the impact of seawater intrusion still gets worse in the dry season due to the lack of water for pushing down the seawater. Molle, Srijantr, and Promchote (2009) mentioned water shortage is not due to the lack of water but to the oversizing of some irrigation areas with relation to available supply and its viability. According to Nguyen et al. (2008), the method through which salt intrusion occurs is complex and depends on a variety of variables, including the upstream discharge of freshwater, the channel's capacity and morphology, the tides, and the presence of control features like water gates.

4.4 Recommendations on Salinity

4.4.1 Suggestions on Salinity Prevention

Concerning the main BPK River, being a part of the BPK river basin, matters related to water resources management is under the supervision of National Water Resources Commission (NWRC), regards to Water Resources Act in 2018. The BPK river basin has Bang Pakong Dialogue, comprises of a wide range of key stakeholders: BPK river basin committee, local administrative bodies, civil society, local NGOs, and government officials. The suggestions for the salinity prevention can be presented in two main parts: (a) Capability within local community and administrative body and (b) Capability of national level.

(a) Capability within local community and administrative body

Based on the results of this research, the downstream has high salinity and thus, for the agricultural areas located near the downstream part, high salt tolerant variation of crops are suggested. It is because salinity had a negative impact on crop yields of rice (Grattan et al., 2002); thus, it is recommended to cultivate genetically modified salt tolerant rice species as the BPK area is mainly focused on agriculture. In addition, it is recommended not to cultivate salinity sensitive plants, for instance, peas, beans and sugarcane, due to the potential of future salinity increment even in the upstream part. As the area needs water for various applications in addition to agriculture, saltwater can be used for cooling in thermoelectric power plant for industrial usage, as there is also a power plant near the Bang Pakong Estuary, operated by EGAT since 1985 (EGAT, 1985). For drinking purposes, desalination can be used to treat saline water into drinking quality (WHO, 2011). Meanwhile in this study area, the salinity problem is linked with the imbalance of water demand and supply due to high agricultural activities, economic benefits analysis, i.e., cost and benefit analysis needs to be conducted in the future. Moreover, strategies that use less water (decreasing demand) while improving rice productivity (Singh et al, 2021), for example improved cultivation practices and salt-tolerant varieties can overcome the deadlock facing in BPK area.

Through collaborating with local research institutes, the study on the impact of human-induced contributions such as the operation of dams from upper river basin

and land use changes, on the salinity issue are highly endorsed. Furthermore, with the aids from Asian Development Bank that already has the cooperation with BPK basin committee, the committee can initiate small projects on plantation of salt-tolerant pasture grass species and fodder shrubs in salt-affected areas, that can be managed by the local community. On the top of that, promoting the cooperation among key stakeholders can overcome obstacles toward salinity management, in particular, lack of knowledge and integration at the local administration, different levels of understanding among government officials, lack of coordination at provincial level, and doubts on the performance of officials by civil society. Thus, building trust and cooperation, starting with small projects such as plantation of salt tolerant grass in salt affected areas can overcome the existing obstacles and promote the salinity management in the BPK area as it is anticipated that salinity will increase in the future based on the time series results.

(b) Capability of national level

As the national level has the sole authority to approve the water budget and associated projects, the assistance from the national level is needed for the tackling the salinity problem of BPK river. When looking back to past government's budget spending on water in Thailand, water budget was amounted to 52.63, 54.2, 60.36, and 62.83 billion baht in 2016, 2017, 2018, and 2019 respectively. For 2021 Financial Year (FY), the government had spent more than 115.44 billion baht on 26,810 water management projects. It is observed that in the present 2022 FY, the Office of the National Water Resources had granted 11,524 projects from 23 agencies, in terms of 1.57 billion baht. Despite the annual increase in budget allocation to solve water-related challenges, there are still emerging water associated issues, for this case, annual increase in salinity in dry season. This highlights the necessities to efficiently allocate public money on confronting emerging water challenges. It is also required to take account on the future climate change, as the country is ranked 9th globally in terms of climate risk (Global Climate Risk Index, 2021). Thus, it is also suggested to integrate climate stress test on evaluating water proposals (European Central Bank, 2021).

Based on the outcome of remote sensing work suggests the need of real time monitoring on salinity is desired. In order to do real time monitoring a research centre or employing technicians at the existing institute is need, that can only be successful with proper budget allocation from the national level. For the real time monitoring, it is learnt that the use of random forest algorithm can efficiently detect the salinity of the river.

Inclusively, when considering management options for BPK area, decisions should be inclusive enough and should take account of salinity issues (variation and distribution), area specific factors (soil, geomorphology, climate), economic significance (value of land and crop production vs implementation cost) and stakeholder opinions.

4.4.2 Limitation of Research

There are some research methodology limitations on salinity issue of BPK river. In term of remote sensing, this study took account only Landsat images, however there are a number of satellites images—Sentinel and MODIS that can provide information similar to Landsat images. On top of that, in relation to machine learning methods, this study uses only four algorithms, namely, multilinear regression (MLR), decision trees (DT), random forest (RF) and artificial neural networks (ANN), in addition to these methods, support vector machines (SVM), self-organizing map (SOM), ensemble methods can be applied. There are very few field measurements taken during the Landsat picture acquisition times due to the revisit frequency of the satellite used in the current study and the requirements of cloud-free circumstances for satellite measurements, especially in the tropical area. Only using Landsat imagery for salinity alerts may make them less effective at protecting the BPK region's agriculture from salinity damage.

Regarding the time series application, only two time series methods—SARIMA and NARNET are employed. However, there are plenty of time series methods such as NARX (Nonlinear autoregressive exogenous model) network is a dynamical neural architecture commonly used for input–output modelling of nonlinear dynamical systems. As time series models are dependent on historical data,

a longer duration of data can generate a better result, i.e., the data needs to be improved by using longer duration for instance 30 years.

Recent advances in numerical simulation, calibration and optimization techniques require rigorous field-scale application to contemporary issues of climate change, socioeconomic and ecological factors that are inseparable elements of saline intrusion management. It needs to be pointed out that there are many contributing factors affecting salinity distribution in the BPK in different seasons. Therefore, direct and indirect connections between the hydro-meteorological factors (i.e., run-off, precipitation, etc.) and anthropogenic factors (i.e., the watergate operation, land-use, and river/coastal management) should be further and thoroughly investigated. Concerning parameters for further studies: river discharge, record of water release from upper basin dams, flooding events, water demand and supply should be included. For instance, Urat and Kanasut applied a hydrodynamic MIKE 11 model for salinity intrusion analysis in the BPK river by considering the effects of run-off and the watergate management on salinity pollution (Urat and Kanasut, 2020). Moreover, investigation of the water gate operations for both seawater intrusion into the river and store freshwater during dry season usage along the BPK River Basin should be more addressed.

The most important aspect of this study is it focus only on the BPK river; however, it is not sufficient to draw salinity management plan without considering the soil salinity along the riverbanks, in particular root zone salinity, and adjacent lands that are mostly agricultural fields. Moreover, testing the salt tolerance of plant, i.e., paddy and genetic modification of paddy to be salt tolerant and the selection of other suitable crops on cultivation, especially for BPK area. In addition, the impact of salinity on the irrigation system as well as investigation salinity intrusion on aquifer should be conducted. Based on the above findings, the following key points should be more considered and further explored:

1. Investigating water demand and supply, in particular focused on water consumption of agricultural uses.
2. Human-induced factors such as upper river basin's dam operations and land use change influence on salinity.

3. Future climate change related impacts on salinity intrusion and water quality of the BPK river basin.
4. Interlinkage between coastal and river basin management of the BPK River.
5. Stakeholders' analysis and vulnerability assessment (i.e., habitat vulnerability, livelihood vulnerability, species vulnerability, etc.) along the BPK River.



CHAPTER 5

CONCLUSION

In accessing the nature of salinity, a statistical model plays a vital role to optimize the calculation. Among the models, the Random Forest (RF) generates the best parameters and proved to maximize the capacity of studying the relationship between the reflectance and salinity. In addition, among the Landsat 8 bands, it is proved that band 2, band 3, band 4 and band 7 are critical for the building up a successful reflectance (wavelength) and salinity model. Moreover, in this type of study that needs a comprehensive sample size, however it is almost impossible to get such a sample covering the detail of the area, bootstrap method is a solution, and it also overcomes the overfitting problem. Thus, this study proves that the Random Forest and bootstrap methods are powerful enough to deal with the insufficient or large area of study in assessing the salinity problem. In addition, based on the result of mapping, different levels of salinity are observed along the river, which can generally divide into four major areas: downstream of BPK, upstream of BPK, tributary of Nakon Nayok, and tributary of Prachin Buri. Out of these four segments, the downstream portion of BPK demonstrates seasonal fluctuations and has the highest salinity. In terms of months, November having the lowest salinity and February having the highest salinity. From the time-sequence salinity maps of BPK river, the annual changes in the salinity can be observed and it can be considered that the variation is more noticeable in the downstream of the BPK river, especially to BPK9.5 (nearby of Bang Pakong Watergate). A similar trend of increasing salinity is observed in predicted value of salinity from SARIMA and NARNET. Based on the forecasted salinity values of SARIMA, maximum and minimum salinity of downstream part in February 2024 is 63.57 - 14.01 dS/m, while in the upstream part, the range of 16.94 - 1.44 dS/m is observed. The area's low-lying topography with an elevation of less than roughly 10 m, contributes to the increase in salinity by allowing saline water to enter the river. However, due to the revisit frequency of the satellite used in the present study and the requirements of cloud-free conditions for satellite measurements especially in the tropical area, there are very limited field measurements acquired during Landsat image acquisition times. Salinity alerts, solely

based on Landsat images may be less useful in preventing salinity damage to agriculture of BPK area.

On the other hand, in terms of parameters that influence the salinity, precipitation and salinity correlation, in terms of EC: Pearson Correlation is -0.170 (p-value < 0.05) and TDS: Pearson Correlation is -0.149 (p-value < 0.05). In addition, temperatures of both water and atmosphere have fair correlations: 0.22 for air (p-value < 0.05) and 0.1 for water (p-value < 0.05) with EC and 0.29 for air (p-value < 0.05) and 0.14 for water (p-value < 0.05). However, the water level has no relationship with the salinity, in which Pearson correlation value is 0.01 with EC and -0.02 with TDS respectively, i.e., water level is not statistically significant. The previous research suggested that stream discharge is more relevant parameter in investigating the relation with salinity, compared to stream level, which can be affected by the streambed due to sedimentation, in which sedimentation might be another influencing factor.

The suggestions for the salinity prevention can be presented in two main parts: (a) Capability within local community and administrative body and (b) Capability of national level. Grounded on the results of this research, the downstream has high salinity and thus, for the agricultural areas located near the downstream part, high salt tolerant variation of crops are suggested. It is because salinity had a negative impact on crop yields of rice (Grattan et al., 2002); thus, it is recommended to cultivate genetically modified salt tolerant rice species as the BPK area is mainly focused on agricultural activities. Meanwhile in this study area, the salinity problem is linked with the imbalance of water demand and supply due to high agricultural activities, economic benefits analysis, i.e., cost and benefit analysis needs to be conducted in the future. Moreover, strategies that use less water (decreasing demand) while improving rice productivity (Singh et al, 2021), for example improved cultivation practices and salt-tolerant varieties can overcome the deadlock facing in BPK area. Through collaborating with local research institutes, the study on the impact of human-induced contributions such as the operation of dams from upper river basin and land use changes, on the salinity issue are highly endorsed. On the top of that, promoting the cooperation among key stakeholders can overcome obstacles toward salinity management as it is anticipated that salinity will increase in the future based on the

time series results. As the national level has the sole authority to approve the water budget and associated projects, the assistance from the national level is needed for the tackling the salinity problem of BPK river. When looking back to past government's budget spending on water in Thailand, water budget was amounted to 52.63, 54.2, 60.36, and 62.83 billion baht in 2016, 2017, 2018, and 2019 respectively. Despite the annual increase in budget allocation to solve water-related challenges, there are still emerging water associated issues, for this case, annual increase in salinity in dry season. This highlights the necessities to efficiently allocate public money on confronting emerging water challenges. It is also required to take account on the future climate change, as the country is ranked 9th globally in terms of climate risk (Global Climate Risk Index, 2021). Thus, it is also suggested to integrate climate stress test on evaluating water proposals (European Central Bank, 2021). Based on the outcome of remote sensing work suggests the need of real time monitoring on salinity is desired. For the real time monitoring, it is learnt that the use of random forest algorithm can efficiently detect the salinity of the river.

Based on the above findings, four key points should be more considered and further explored: (a) Investigating water demand and supply, in particular focused on water consumption of agricultural uses, (b) Human-induced factors such as upper river basin's dam operations and land use change influence on salinity, (c) Future climate change related impacts on salinity intrusion and water quality of the BPK river basin, (d) Interlinkage between coastal and river basin management of the BPK River and (e) Stakeholders' analysis and vulnerability assessment (i.e., habitat vulnerability, livelihood vulnerability, species vulnerability, etc.) along the BPK River.

REFERENCES



จุฬาลงกรณ์มหาวิทยาลัย
CHULALONGKORN UNIVERSITY

Acharya, T.D. (2015) 'Exploring Landsat-8', *International Journal of IT, Engineering and Applied Sciences Research*, 4, pp. 4–10.

AL-Allaf, O.N.A. and AbdAlKader, S.A. (2011) 'Nonlinear autoregressive neural network for estimation soil temperature: A comparison of different optimization neural network algorithm', in *IEEE International Conference on Industrial Technology*,. Auburn; USA, pp. 43–51.

Ali Khan, M. et al. (2022) 'Application of random forest for modelling of surface water salinity', *Ain Shams Engineering Journal*, 13(4), p. 101635. Available at: <https://doi.org/10.1016/j.asej.2021.11.004>.

Ansari, M. and Akhoondzadeh, M. (2019) 'Water salinity mapping of karun basin located in iran using the SVR method', *International Archives of the Photogrammetry, Remote Sensing and Spatial Information Sciences - ISPRS Archives*, 42(4/W18), pp. 97–101. Available at: <https://doi.org/10.5194/isprs-archives-XLII-4-W18-97-2019>.

Ansari, M. and Akhoondzadeh, M. (2020) 'Mapping water salinity using Landsat-8 OLI satellite images (Case study: Karun basin located in Iran)', *Advances in Space Research*, 65(5), pp. 1490–1502. Available at: <https://doi.org/10.1016/j.asr.2019.12.007>.

Basu, A. and Basu, Si. (2011) *Decision Trees: A User Guide to Business Analytics*. New York: Talyer & Francis Group.

Bordalo, A A, Nilsumranchit, W. and Chalermwat, K. (2001) 'Water Quality and Uses of the Bang Pakong River, Eastern Thailand', *Wat. Res*, 35(15), pp. 3635–3642.

Bordalo, A. A., Nilsumranchit, W. and Chalermwat, K. (2001) 'Water quality and uses of the Bangpakong River (Eastern Thailand)', *Water Research*, 35(15). Available at: [https://doi.org/10.1016/S0043-1354\(01\)00079-3](https://doi.org/10.1016/S0043-1354(01)00079-3).

Breiman, L. (2001) 'Random Forests', *Machine Learning*, 45, pp. 5–32. Available at: https://doi.org/10.1007/978-3-030-62008-0_35.

Bubphamala, T., Benjawan, L. and Liamlaem, W. (2010) 'Seasonal Variations of Water Quality in Bangpakong River and Nearby Canals at Banpho District', *Kasetsart Journal - Natural Science*, 44(4), pp. 732–743.

Chaiyarak, B., Tattiyakul, G. and Karnsunthad, N. (2019) *Climate Change Vulnerability Assessment Bang Pakong River Wetland, Thailand*.

Chan, R. et al. (2020) 'Fate, Transport and Ecological Risk of Antibiotics from Pig Farms along the Bang Pakong River, Thailand', *Agriculture, Ecosystems and Environment*, 304(July), p. 107123. Available at: <https://doi.org/10.1016/j.agee.2020.107123>.

Constantin, S., Constantinescu, S. and Doxaran, D. (2017) 'Long-term Analysis of Turbidity Patterns in Danube Delta Coastal Area Based on MODIS Satellite Data', *Journal Marine System*, 170, pp. 10–21.

Dixon, P.M. (2001) 'Bootstrap Resampling', *Encyclopedia of Environmetrics* [Preprint]. Available at: <https://doi.org/10.1002/9780470057339.vab028>.

Dixon, P.M. (2006) 'Bootstrap Resampling', in *Encyclopedia of Environmetrics*, pp. 212–220. Available at: <https://doi.org/10.1002/9780470057339.vab028>.

Epifanio, I. (2017a) 'Intervention in prediction measure: A new approach to assessing variable importance for random forests', *BMC Bioinformatics*, 18(1), pp. 1–16. Available at: <https://doi.org/10.1186/s12859-017-1650-8>.

Epifanio, I. (2017b) 'Intervention in prediction measure: A new approach to assessing variable importance for random forests', *BMC Bioinformatics*, 18(1), pp. 1–16. Available at: <https://doi.org/10.1186/s12859-017-1650-8>.

Fang, L. et al. (2010) 'Detecting Marine Intrusion into Rivers Using EO-1 ALI Satellite Imagery: Modern Waterway, Pearl River Estuary, China', *International Journal of Remote Sensing*, 31, pp. 4125–4146.

Fassnacht, F.E. et al. (2014) 'Importance of sample size, data type and prediction method for remote sensing-based estimations of aboveground forest biomass', *Remote Sensing of Environment*, 154(1). Available at: <https://doi.org/10.1016/j.rse.2014.07.028>.

Hadiyan, P.P., Moeini, R. and Ehsanzadeh, E. (2020) 'Application of static and dynamic artificial neural networks for forecasting inflow discharges, case study: Sefidroud Dam reservoir', *Sustainable Computing: Informatics and Systems*, 27, p. 100401. Available at: <https://doi.org/10.1016/j.suscom.2020.100401>.

Hastie, T., Tibshirani, R. and Friedman, J. (2009) *The Elements of Statistical Learning: Data Mining, Inference and Prediction*. Springer S. California: Springer.

Haukoos, J.S. and Lewis, R.J. (2005) 'Advanced Statistics: Bootstrapping Confidence Intervals for Statistics with “Difficult” Distributions', *Academic Emerging Medicine*, 12(4), pp. 360–365. Available at: <https://doi.org/10.1197/j.aem.2004.11.018>.

Hayashi, M. (2004) 'Temperature-electrical conductivity relation of water for environmental monitoring and geophysical data inversion', *Environmental Monitoring and Assessment*, 96(1–3), pp. 119–128. Available at: <https://doi.org/10.1023/B:EMAS.0000031719.83065.68>.

Himi, M. et al. (2017) 'Geophysical characterization of saltwater intrusion in a coastal aquifer: The case of Martil-Alila plain (North Morocco)', *Journal of African Earth Sciences*, 126, pp. 136–147. Available at: <https://doi.org/10.1016/j.jafrearsci.2016.11.011>.

- Hipel, K.W., McLeod, A.I. and Lennox, W.C. (1977) 'Advances in Box-Jenkins Modeling', *Water Resources Research*, 13(3), pp. 567–575.
- Ibrahim, M. et al. (2014) 'Energy management for a fuel cell hybrid electrical vehicle', in 40th Annual Conference of the IEEE Industrial Electronics Society, IECON, pp. 3955–3961. Available at: <https://doi.org/10.1109/IECON.2014.7049092>.
- Ibrahim, M. et al. (2016) 'Nonlinear autoregressive neural network in an energy management strategy for battery/ultra-capacitor hybrid electrical vehicles', *Electric Power Systems Research*, 136, pp. 262–269. Available at: <https://doi.org/10.1016/j.epsr.2016.03.005>.
- Katsaros, K. and Buettner, K.J.K. (1969) 'Influence of Rainfall on Temperature and Salinity of the Ocean Surface', *Journal of Applied Meteorology*, 8(1). Available at: [https://doi.org/10.1175/1520-0450\(1969\)008<0015:iorota>2.0.co;2](https://doi.org/10.1175/1520-0450(1969)008<0015:iorota>2.0.co;2).
- Kbaier Ben Ismail, D., Lazure, P. and Puillat, I. (2016) 'Statistical properties and time-frequency analysis of temperature, salinity and turbidity measured by the MAREL Carnot station in the coastal waters of Boulogne-sur-Mer (France)', *Journal of Marine Systems*, 162, pp. 137–153. Available at: <https://doi.org/10.1016/j.jmarsys.2016.03.010>.
- Kumar, D.N. and Reshmidevi, T.V. (2013) 'Remote Sensing Applications in Water Resources', *Journal Indian I Science*, 93, pp. 163–187.
- Kunacheva, C. et al. (2009) 'Contamination of perfluorinated compounds (PFCs) in Chao Phraya River and Bangpakong River, Thailand', *Water Science and Technology*, 60(4), pp. 975–982. Available at: <https://doi.org/10.2166/wst.2009.462>.
- Kupkanchanakul, W. et al. (2015) 'Integrating Spatial Land Use Analysis and Mathematical Material Flow Analysis for Nutrient Management: A Case Study of the Bang Pakong River Basin in Thailand', *Environmental Management*, 55(5), pp. 1022–1035. Available at: <https://doi.org/10.1007/s00267-014-0441-5>.
- Lapedes, A. and Farber, R. (1987) *Nonlinear Signal Processing Using Neural Network: Prediction and Modeling*. New Mexico.
- Lin, T. et al. (1996) 'Learning Long-Term Dependencies in NARX Recurrent Neural Networks', *IEEE Transactions on Neural Networks*, 7(6), pp. 1329–1338.
- Loc, H.H. et al. (2021) 'Intensifying saline water intrusion and drought in the Mekong Delta: From physical evidence to policy outlooks', *Science of the Total Environment*, 757, p. 143919. Available at: <https://doi.org/10.1016/j.scitotenv.2020.143919>.
- Lorek, K.S. et al. (1976) 'Earnings Linked references are available on JSTOR for this article: A Comparative Examination of Management Forecasts and Box-Jenkins Forecasts of Earnings', 51(2), pp. 321–330.

- Ma, H., Guo, S. and Zhou, Y. (2013) 'Detection of Water Area Change Based on Remote Sensing Images', in Proceedings of Geo-informatics in Resource Management and Sustainable Ecosystem, Part 1. Wuhan, China.
- MacKinnon, J. (2007) Bootstrap Hypothesis Testing, Queens's Economics Department Working Paper. Available at: <https://doi.org/10.1111/j.1467-842X.1990.tb01011.x>.
- McFeeters, S.K. (1996) 'The use of the Normalized Difference Water Index (NDWI) in the delineation of open water features', *International Journal of Remote Sensing*, 17(7), pp. 1425–1432. Available at: <https://doi.org/10.1080/01431169608948714>.
- McPherson, J.M., Jetz, W. and Rogers, D.J. (2004) 'The effects of species' range sizes on the accuracy of distribution models: Ecological phenomenon or statistical artefact?', *Journal of Applied Ecology*, 41(5), pp. 811–823. Available at: <https://doi.org/10.1111/j.0021-8901.2004.00943.x>.
- Messner, J.W., Mayr, G.J. and Zeileis, A. (2017) 'Nonhomogeneous boosting for predictor selection in ensemble postprocessing', *Monthly Weather Review*, 145(1). Available at: <https://doi.org/10.1175/MWR-D-16-0088.1>.
- Molle, F., Srijantr, T. and Promchote, P. (2009) The Bang Pakong River Basin Committee: Analysis and Summary of Experience. Bangkok.
- Morgan, R.S., El-Hady, M.A. and Rahim, I.S. (2018) 'Soil salinity mapping utilizing sentinel-2 and neural networks', *Indian Journal of Agricultural Research*, 52(5), pp. 524–529. Available at: <https://doi.org/10.18805/IJARE.A-316>.
- Nguyen, A.D. et al. (2008) 'Using salt intrusion measurements to determine the freshwater discharge distribution over the branches of a multi-channel estuary: The Mekong Delta case', *Estuarine, Coastal and Shelf Science*, 77(3), pp. 433–445. Available at: <https://doi.org/10.1016/j.ecss.2007.10.010>.
- Nguyen, P.T.B. et al. (2018) 'Remote sensing techniques to predict salinity intrusion: application for a data-poor area of the coastal Mekong Delta, Vietnam', *International Journal of Remote Sensing*, 39(20). Available at: <https://doi.org/10.1080/01431161.2018.1466071>.
- Nguyen, T.B.P. (2018) Remote Sensing Application for Assessing Salinity Intrusion in Mekong Delta, Vietnam. Prince Songkla University.
- Nguyen, T.G. et al. (2021) 'Salinity intrusion prediction using remote sensing and machine learning in data-limited regions: A case study in Vietnam's Mekong Delta', *Geoderma Regional*, 27(May), p. e00424. Available at: <https://doi.org/10.1016/j.geodrs.2021.e00424>.
- Niu, B. et al. (2019a) 'A novel neural-network-based adaptive control scheme for output-constrained stochastic switched nonlinear systems', *IEEE Transactions on*

Systems, Man, and Cybernetics: Systems, 49(2), pp. 418–432. Available at: <https://doi.org/10.1109/TSMC.2017.2777472>.

Niu, B. et al. (2019b) ‘A novel neural-network-based adaptive control scheme for output-constrained stochastic switched nonlinear systems’, IEEE Transactions on Systems, Man, and Cybernetics: Systems, 49(2). Available at: <https://doi.org/10.1109/TSMC.2017.2777472>.

Notton, G. and Voyant, C. (2018) ‘Forecasting of Intermittent Solar Energy Resource’, in *Advances in Renewable Energies and Power Technologies*. Elsevier Inc., pp. 77–114. Available at: <https://doi.org/10.1016/B978-0-12-812959-3.00003-4>.

Ouma, Y.O., Okuku, C.O. and Njau, E.N. (2020) ‘Use of Artificial Neural Networks and Multiple Linear Regression Model for the Prediction of Dissolved Oxygen in Rivers: Case Study of Hydrographic Basin of River Nyando, Kenya’, *Complexity*, 2020. Available at: <https://doi.org/10.1155/2020/9570789>.

Owen, A.B. (2001) Chapter 4: Empirical Likelihood in Regression and Modeling. New York: Chapman and Hall.

Peddle, D.R. et al. (2001) ‘Reflectance processing of remote sensing spectroradiometer data’, *Computers and Geosciences*, 27(2), pp. 203–213. Available at: [https://doi.org/10.1016/S0098-3004\(00\)00096-0](https://doi.org/10.1016/S0098-3004(00)00096-0).

Preacher, K.J. and Hayes, A.F. (2008) ‘Asymptotic and resampling strategies for assessing and comparing indirect effects in multiple mediator models’, *Behavior Research Methods*, 40(3), pp. 879–891. Available at: <https://doi.org/10.3758/BRM.40.3.879>.

Promchote, P. (2009) The Bang Pakong River Basin Committee: analysis and summary of experience.

Rhoades, J.D., Kandiah, A. and Mashali, A.M. (2012) ‘The use of saline waters for crop production - FAO irrigation and drainage paper 48’, *FAO Irrigation and Drainage Paper* [Preprint].

Rouchier, S., Rabouille, M. and Oberlé, P. (2018) ‘Calibration of simplified building energy models for parameter estimation and forecasting: Stochastic versus deterministic modelling’, *Building and Environment*, 134(March), pp. 181–190. Available at: <https://doi.org/10.1016/j.buildenv.2018.02.043>.

Roy, D.P. et al. (2014) ‘Landsat-8: Science and Product Vision for Terrestrial Global Change Research’, *Remote Sensing of Environment*, 145, pp. 154–172.

Sawaya, K.E. et al. (2003) ‘Extending Satellite Remote Sensing to Local Scales: Land and Water Resource Monitoring Using High-resolution Imagery’, *Remote Sensing of Environment*, 88, pp. 144–156.

Shehhi, M.R. and Kaya, A. (2021) 'Time series and neural network to forecast water quality parameters using satellite data', *Continental Shelf Research*, 231(July 2020), p. 104612. Available at: <https://doi.org/10.1016/j.csr.2021.104612>.

Stephen, M. (2007) Part V: Intelligent System - Machine Learning in Computing Handbook Computer Science and Software Engineering. Boca Raton: Chapman and Hall.

Stockwell, D.R.B. and Peterson, A.T. (2002) 'Effects of sample size on accuracy of species distribution models', *Ecological Modelling*, 148(1), pp. 1–13. Available at: [https://doi.org/10.1016/S0304-3800\(01\)00388-X](https://doi.org/10.1016/S0304-3800(01)00388-X).

Temurtas, F. et al. (2004) 'Harmonic detection using feed forward and recurrent neural networks for active filters', *Electric Power Systems Research*, 72(1), pp. 33–40. Available at: <https://doi.org/10.1016/j.epr.2004.02.005>.

Tran, T. V. et al. (2019) Examining spatiotemporal salinity dynamics in the Mekong River Delta using Landsat time series imagery and a spatial regression approach, *Science of the Total Environment*. Elsevier B.V. Available at: <https://doi.org/10.1016/j.scitotenv.2019.06.056>.

Tran, T.A. et al. (2021) 'Moving towards sustainable coastal adaptation: Analysis of hydrological drivers of saltwater intrusion in the Vietnamese Mekong Delta', *Science of the Total Environment*, 770, p. 145125. Available at: <https://doi.org/10.1016/j.scitotenv.2021.145125>.

Trung, N.H. and Tri, V.P.D. (2014) 'Possible Impacts of Seawater Intrusion and Strategies for Water Management in Coastal Areas in Vietnamese Mekong Delta in the Context of Climate Change', *Coastal Disasters and Climate Change in Vietnam [Preprint]*.

Tunjung, D.M. et al. (2021) 'Estuary zone based on sea level salinity in Ciletuh Bay, West Java', *IOP Conference Series: Earth and Environmental Science*, 623(1). Available at: <https://doi.org/10.1088/1755-1315/623/1/012083>.

UC Berkeley (2008) 'Landsat Spectral Band Information', Reference, 6, pp. 6–7.

Urquhart, E.A. et al. (2012) 'Remotely Sensed Estimates of Surface Salinity in the Chesapeake Bay: A Statistical Approach', *Remote Sensing of Environment*, 123, pp. 522–531.

Urat W, Kanasut J. Salinity intrusion analysis in Bangpakong River by Mathematical Model MIKE 11. The 13th Thai National Committee on Irrigation and Drainage (Thai CID) National Symposium, 2020

U.S. Geological Survey (2019) 'Landsat 8 Data Users Handbook', Nasa, 8(November), p. 114.

Valbuena, R., Maltamo, M. and Packalen, P. (2016) 'Clasificación de etapas de desarrollo forestal a partir de datos de vuelos lidar nacionales de baja densidad:

Comparación de métodos de aprendizaje automático’, *Revista de Teledeteccion*, 2016(45), pp. 15–25. Available at: <https://doi.org/10.4995/raet.2016.4029>.

Valipour, M., Banihabib, M.E. and Behbahani, S.M.R. (2013) ‘Comparison of the ARMA, ARIMA, and the autoregressive artificial neural network models in forecasting the monthly inflow of Dez dam reservoir’, *Journal of Hydrology*, 476, pp. 433–441. Available at: <https://doi.org/10.1016/j.jhydrol.2012.11.017>.

Vanhellemont, Q. and Ruddick, K. (2014) ‘Landsat-8 As a Precursor To Sentinel-2: Observations of Human Impacts in Coastal Waters’, in *Proceedings of the Sentinel-2 for Science Workshop (2008)*. Frascati, ESA Italy.

Vongvisessomjai, S., Chatanantavet, P. and Srivihok, P. (2008) ‘Interaction of Tide and Salinity Barrier: Limitation of Numerical Model’, *Songklanakarin Journal of Science and Technology*, 30(4), pp. 531–538.

Vongvisessomjai, S. and Srivihok, P. (2003) ‘The Interaction between Tide and Salinity Barriers’, *Songklanakarin Journal of Science and Technology*, 25(6), pp. 743–756.

Wang, F. and Xu, Y.J. (2008) ‘Development and Application of a Remote Sensing-based Salinity Prediction Model for a Large Estuarine Lake in the US Gulf of Mexico Coast’, *Journal of Hydrology*, 360, pp. 184–194.

Wang, F. and Xu, Y.J. (2008) ‘Development and application of a remote sensing-based salinity prediction model for a large estuarine lake in the US Gulf of Mexico coast’, *Journal of Hydrology*, 360(1–4). Available at: <https://doi.org/10.1016/j.jhydrol.2008.07.036>.

Wassmann, R. et al. (2019) ‘High-resolution mapping of flood and salinity risks for rice production in the Vietnamese Mekong Delta’, *Field Crops Research*, 236(April), pp. 111–120. Available at: <https://doi.org/10.1016/j.fcr.2019.03.007>.

Wehrens, R., Putter, H. and Buydens, L.M.C. (2000) ‘The bootstrap: A tutorial’, *Chemometrics and Intelligent Laboratory Systems*, 54(1), pp. 35–52. Available at: [https://doi.org/10.1016/S0169-7439\(00\)00102-7](https://doi.org/10.1016/S0169-7439(00)00102-7).

Wei, W.W.S. and Hillmer, S.C. (1991) ‘Time Series Analysis: Univariate and Multivariate Methods’, *Journal of American Statistical Association*, 86(413), pp. 245–246.

Weijis, S. v., Mutzner, R. and Parlange, M.B. (2013) ‘Could electrical conductivity replace water level in rating curves for alpine streams?’, *Water Resources Research*, 49(1). Available at: <https://doi.org/10.1029/2012WR012181>.

Xiao, H. et al. (2018) ‘Assessing sea-level rise impact on saltwater intrusion into the root zone of a geo-typical area in coastal east-central Florida’, *Science of the Total Environment*, 630, pp. 211–221. Available at: <https://doi.org/10.1016/j.scitotenv.2018.02.184>.

Xiong, Y. et al. (2012) 'The Impacts of Rapid Urbanization on the Thermal Environment: A Remote Sensing Study of Guangzhou, South China', *Remote Sensing*, 4(7), pp. 2033–2056. Available at: <https://doi.org/10.3390/rs4072033>.

Zhao, J., Temimi, M. and Ghedira, H. (2017) 'Remotely Sensed Sea Surface Salinity in the Hyper-saline Arabian Gulf: Application of Landsat-8 OLI Data', *Estuarine, Coastal and Shelf Science*, 187, pp. 168–177.



ANNEX

Annex 1: Thermal Infrared Sensor (TIRS) and Operational Land Imager (OLI) Source Wavelengths for Landsat 8 (U.S. Geological Survey, 2019)

Band Number	Band Name	Wavelength (μm)	Resolution (m)
Band 1	Ultra-Blue (Coastal/aerosol)	0.43 – 0.45	30
Band 2	Blue	0.45 – 0.51	30
Band 3	Green	0.53 – 0.59	30
Band 4	Red	0.64 – 0.67	30
Band 5	Near Infrared (NIR)	0.85 – 0.88	30
Band 6	Shortwave Infrared (SWIR 1)	1.57 – 1.65	30
Band 7	Shortwave Infrared (SWIR 2)	2.11 – 2.29	30
Band 8	Panchromatic	0.50 – 0.68	15
Band 9	Cirrus	1.36 – 1.38	30
Band 10	Thermal Infrared (TIRS 1)	10.60 – 11.19	100 * (30)
Band 11	Thermal Infrared (TIRS 2)	11.50 -12.51	100 * (30)



Annex 2: Location of stations and grouping based on Time Series Methods

Name	Distinct Feature	Sub-district	District	Latitude	Longitude	Grouping: SARIMA	Grouping: NARNET
BK01	Pier	Tha Kham	Bang Pakong	13.47589	100.9821	Group 1	Group 1
BK02	Restaurant	Tha Kham	Bang Pakong	13.48516	101.0027	Group 2	Group 1
BK03	Bridge	Tha Sa An	Bang Pakong	13.54853	101.0008	Group 3	Group 1
BK04	Bridge	Sanam Chan	Ban Pho	13.59988	101.0764	Group 2	Group 1
BK06	Bridge	Bang Phra	Mueang Chachoengsao	13.65937	101.0631	Group 4	Group 2
BK07	Bridge	Na Mueang	Mueang Chachoengsao	13.68801	101.0772	Group 4	Group 2
BK08	School	Ban Mai	Mueang Chachoengsao	13.69982	101.1088	Group 4	Group 2
BK09	Bridge	Bang Kaeo	Mueang Chachoengsao	13.69356	101.1318	Group 4	Group 2
BK9.5	Bridge (Watergate)	Bang Kaeo	Mueang Chachoengsao	13.70713	101.1352	Group 4	Group 2
BK11	Bang Khla Floating Market	Bang Khla	Bang Khla	13.72892	101.2077	Group 5	Group 3
BK13	Wat Hua Sai	Hua Sai	Bang Khla	13.77815	101.2029	Group 5	Group 3
BK15	Bridge	Bang Khanak	Bang Nam Priao	13.87032	101.1459	Group 5	Group 3
BK16	Hospital	Bang Taen	Bang Sang	13.8933	101.1626	Group 5	Group 3

VITA

NAME Min Thura Mon

DATE OF BIRTH 18 May 1997

PLACE OF BIRTH Yangon

INSTITUTIONS ATTENDED University of Yangon

HOME ADDRESS No 83A, Kaymar street, Myoma 2 Ward, Mudon Township, Mon State, Myanmar

PUBLICATION

- (1) Mon, M.T., Piemjaiswang, R., and Kittipongvises, S., (2022) In: 48th International Congress on Science, Technology and Technology-based Innovation, pp 378-385.
- (2) Mon, M.T., et al (2022). In: 11th International Conference on Environmental Engineering, Science and Management. Srisatit, T., Wirojanagud, W., Chotpantararat, S. (Ed.) pp 43-44.
- (3) Mon, M.T., and Zaw, T.N., (2019). In: 1st International Conference and Seminar on Environmental Science and Pollution. Ngwe, H., Than, N.N., Aye, H.H, and Nwe, N. (Ed.) pp 84-115.
- (4) Zaw, T.N., Htet, S.W., and Mon, M.T., (2019). J. Myanmar Acad. Arts Sci. 18 (5), pp 251-282.
- (5) Zaw, T.N., Htet, S.W., and Mon, M.T., (2018). J. Myanmar Acad. Arts Sci. 16 (5), pp 69-105.

AWARD RECEIVED ASEAN and Non-ASEAN Scholarship